NASA TECHNICAL NOTE

NASA TN D-5271

c. 1

NASA TN D-5271

JUPITER SWINGBY MISSIONS TO NONSPECIFIC LOCATIONS IN INTERPLANETARY SPACE

by Jerry M. Deerwester

NASA Headquarters
Mission Analysis Division
Moffett Field, Calif.

NATIONAL AERONAUTICS AND SPACE ADMINISTRATION • WASHINGTON, D. C. • JUNE 1969

JUPITER SWINGBY MISSIONS TO NONSPECIFIC LOCATIONS IN INTERPLANETARY SPACE

By Jerry M. Deerwester

NASA Headquarters
Mission Analysis Division
Moffett Field, Calif.

NATIONAL AERONAUTICS AND SPACE ADMINISTRATION

For sale by the Clearinghouse for Federal Scientific and Technical Information
Springfield, Virginia 22151 – CFSTI price $3.00

JUPITER SWINGBY MISSIONS TO NONSPECIFIC LOCATIONS IN INTERPLANETARY SPACE

By Jerry M. Deerwester

NASA Headquarters
Moffett Field, Calif.

SUMMARY

This report describes trajectories based on the Jupiter swingby flight mode that may be appropriate for exploration of interplanetary space. Interplanetary space refers to regions of the solar system that can be characterized by perihelion or aphelion distances, heliocentric inclination, and the like. Trajectories to particular targets (planets, asteroids, or comets) are not considered.

The results for seven values of Earth departure velocity are summarized as a series of contour charts that depict the features of the post-Jupiter encounter trajectories. The coordinate system employed on these charts is inclination of the passage hyperbola at Jupiter and the pericenter distance. The following post-encounter trajectory parameters are illustrated: perihelion and aphelion distances; heliocentric inclinations; and flight times to perihelion, maximum heliocentric latitude, 10 AU, and 50 AU.

It is shown that, within this class of Jupiter swingbys, greater trajectory flexibility in terms of reduced flight times, higher inclinations, etc., is achieved with increasing Earth departure speed.

INTRODUCTION

Spacecraft trajectories to various regions of the solar system will be necessary as part of a flight program to further our knowledge of interplanetary space and to understand the influences of the Sun's activity and of the galactic background on these characteristics. Depending on the nature of the observations to be made, at least one of three general trajectory categories will be appropriate; namely, those with small perihelion radii, those with large aphelion radii (including solar system escape trajectories), or those inclined to the ecliptic plane. It should be noted that these categories are not necessarily mutually exclusive. For a specified Earth departure speed (commonly referred to in the literature as characteristic velocity) and useful spacecraft lifetime, for example, a trajectory may exist that closely approaches the Sun and that is also highly inclined to the ecliptic. The purpose of this report is to aid the mission planner in reaching suitable compromises between mission objectives and system constraints by setting forth, in a broad parametric manner, the characteristics of some possible heliocentric trajectories that are not constrained by specified terminal conditions (i.e., no planetary intercept).

As with all space missions, two distinct trajectory techniques are conceptually available, that is, ballistic and low thrust transfers. This report is concerned only with the use of ballistic transfers. Recent analyses of missions that employ low thrust propulsion systems can be found in references 1-3.

Within the category of ballistic transfers, both direct and planetary swingbys exist. Previous studies (refs. 4-7) have concluded that certain mission categories, if carried out by the direct flight mode, would require Earth departure velocities in excess of foreseen capabilities (e.g., close solar probes and highly inclined heliocentric orbits) or would require inordinately long flight times (e.g., missions to the outermost planets). These same studies, however, have also indicated that such adverse features can be largely overcome if the planetary swingby mode is used. Because of its strong gravitational field and suitable location in the solar system, Jupiter is the most useful of all the planets as the swingby planet for missions of the type considered here. Consequently, this report is concerned solely with Jupiter swingby missions.

Since these missions do not terminate with a planetary intercept, the characteristics (i.e., inclination and pericenter distance) of the passage hyperbola can be chosen to select particular aspects of the subsequent trajectory. For any combination of passage inclination, distance, and Earth departure speed (characteristic velocity), a unique post-encounter trajectory results. If, for each characteristic velocity, the passage conditions (i.e., inclination and distance) are permitted to vary, a set of post-encounter heliocentric trajectories exists. This, then, suggests the form adopted in this report for presentation of the numerical results; namely, contours of relevant post-encounter trajectory parameters plotted in the passage inclination-pericenter distance plane. This manner of presentation also affords the mission planner the opportunity to select passage conditions that, in their own right, may enhance any observations to be carried out near Jupiter itself.

NOMENCLATURE

a	semimajor axis
e	eccentricity
i	heliocentric inclination
$\hat{i},\hat{j},\hat{k}$	unit vectors along x,y,z axes
k	hyperbolic bend angle at Jupiter
m	planetary mass (solar units)
r	distance from Sun
r_{2_4}	distance of Jupiter from Sun at encounter

R	planetary radius
R_p	pericenter distance (planetary radii)
t	transfer time on heliocentric conic
$\overline{V}$	heliocentric orbital velocity of Jupiter, with speed $V = \lvert\overline{V}\rvert$ [1]
V_c	characteristic velocity (Earth departure speed)
$\overline{V}_1$	heliocentric velocity at Jupiter encounter, with speed $V_1 = \lvert\overline{V}_1\rvert$
$\overline{V}_2$	initial heliocentric velocity of post-encounter trajectory, with speed $V_2 = \lvert\overline{V}_2\rvert$
$\overline{V}_\infty$	hyperbolic excess velocity, with speed $V_\infty = \lvert\overline{V}_\infty\rvert$
x,y,z	rectangular coordinate axes
γ_1	heliocentric path angle at Jupiter encounter
γ_2	initial heliocentric path angle of post-encounter trajectory
Γ	inclination of passage hyperbola
η	heliocentric latitude
θ	heliocentric transfer angle
θ_m	limiting true anomaly on hyperbolic trajectory
θ_o	angle from perihelion at initiation of post-encounter trajectory
$(\hat{})$	unit vector

PHYSICAL MODEL AND ASSUMPTIONS

Inasmuch as the parameters of the post-encounter trajectories are direct functions of both the Earth-Jupiter trajectories and the passage conditions, the features of these last-mentioned phases of the mission are briefly discussed in this section. A representative mission is also discussed to make clear the overall mission profiles and to further define the trajectory parameters. More detailed discussions of the passage geometry and the post-encounter equations of motion are contained in appendixes A and B.

[1] All speeds given in emos (emos is Earth mean orbital speed of 29.8 km/sec).

Earth-Jupiter Trajectories

Opportunities for missions to Jupiter occur every 13 months. Because of Jupiter's small orbital eccentricity and inclination, the trajectory parameters vary but slightly among launch opportunities. For this reason, Earth-Jupiter trajectories are often approximated by assuming that Jupiter's orbit is circular and lies in the ecliptic plane. However, because some variations in velocity and flight time requirements do exist and since the actual requirements are slightly greater than the simplified model would predict, the approach here is first to employ trajectory characteristics associated with a particular launch opportunity; the 1975 opportunity was assumed. The relevant parameters for this opportunity are shown as a function of characteristic velocity in figure 1; the data are from reference 8. It is because of the observed strong dependence of the various trajectory parameters (in particular, the flight time) on the characteristic velocity that characteristic velocity is used as a parameter in analyzing the post-encounter trajectories. The variations in radius and speed of Jupiter's orbit are the result of employing the actual orbital eccentricity in the trajectory calculations. They result from the changing encounter date with V_c. Note also that all Earth-Jupiter trajectories that originate with characteristic velocities greater than 16.5 km/sec are hyperbolic. It will be seen later that the Jupiter passages can yield hyperbolic post-encounter trajectories for all lower values of V_c, and elliptical post-encounter trajectories can be made to occur for higher values of V_c.

Earth-Jupiter trajectory parameters for all other launch opportunities during the 1970 decade were examined to determine the actual variations from those of the 1975 opportunity; trajectories during this period are similar to those that exist during other periods of interest. These variations can be summarized as follows:

- The minimum value of V_c is 14.1 km/sec (1970, 1971 opportunities); the maximum value is 14.6 km/sec (1979 opportunity). The corresponding value for 1975 (from fig. 1) is 14.25 km/sec.

- The shortest flight time associated with minimum V_c is 1.86 years (1973 opportunity); the maximum value is 2.75 years (1980 opportunity). These are to be compared with the value for the 1975 opportunity of 2.19 years.

- As discussed later, the Earth-Jupiter trajectory for which the hyperbolic excess speed at Jupiter is equal to Jupiter's heliocentric orbital speed is significant in the analysis of the post-encounter trajectories. During the 1975 opportunity this trajectory is defined by V_c = 15.6 km/sec. This is a maximum value and is essentially equal during four other opportunities (1974, 1976, 1977, 1980). This trajectory type can be achieved for values of V_c as low as 15.2 km/sec during the 1970 and 1971 opportunities.

Passage Conditions at Jupiter

Having ensured (by not using a circular coplanar model at the outset) that real velocity requirements have been established for any launch

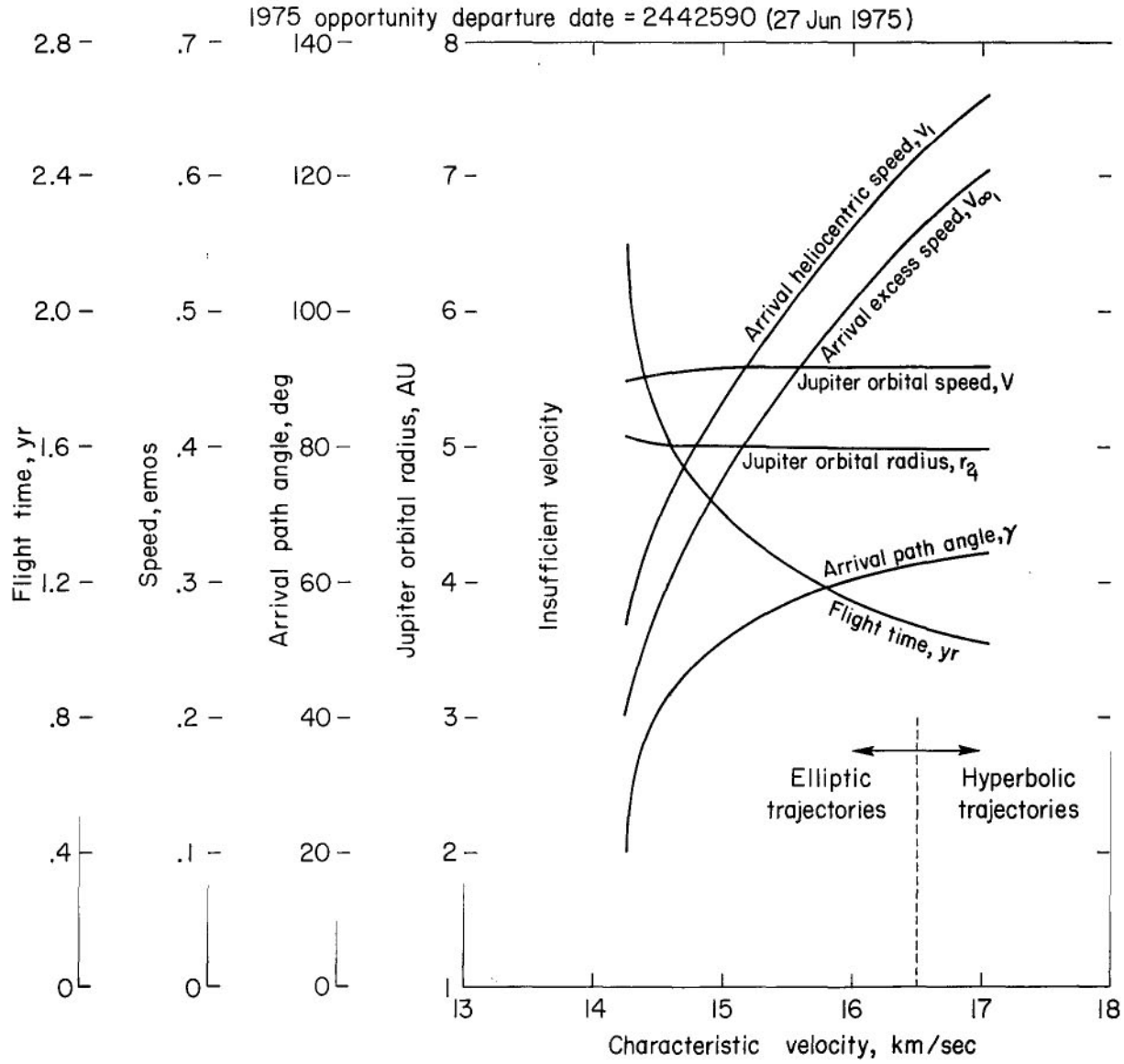

Figure 1.- Earth-Jupiter trajectory characteristics.

vehicle/upper stage combination and that the corresponding flight times are accurate, we then assume a simplified model for the analysis of the passage conditions because it considerably simplifies the analysis. The justification for this assumption is that the actual values of Jupiter's path angle and inclination are small compared with the possible changes in path angle and inclination of the trajectory as measured before and after encounter.

The simplified model assumes (1) that the orbital planes of Jupiter and the Earth-Jupiter trajectory are coincident with the ecliptic plane, (2) that Jupiter's orbit at encounter is characterized by zero path angle with the heliocentric distance and speed as shown in figure 1, and (3) that Jupiter's equatorial plane is also coincident with the ecliptic. This last assumption is justifiable since Jupiter's obliquity is only 3°. It is desirable because it makes the post-encounter trajectory possibilities symmetric about the Jupiter equatorial plane.

Mission Profiles

Figure 2 illustrates the essential characteristics of the Jupiter swingby missions. The example shown is an out-of-ecliptic/solar probe mission. The spacecraft is launched from Earth and transfers in the ecliptic plane to Jupiter. Just prior to entering Jupiter's sphere of influence (i.e., before Jupiter's gravitational acceleration significantly perturbs the spacecraft trajectory), the heliocentric velocity of the spacecraft is $\overline{V}_1$ and the path angle is γ_1, measured in the plane of heliocentric motion between the normal to the Sun-Jupiter radius vector and the heliocentric velocity vector. At the sphere of influence, the hyperbolic excess approach velocity vector is defined as $\overline{V}_\infty = \overline{V}_1 - \overline{V}$.

After emerging from the sphere of influence, the post-encounter trajectory has initial heliocentric velocity $\overline{V}_2$ and path angle γ_2, where $\overline{V}_2 = \overline{V} + \overline{V}_{\infty_2}$. Since there are no propulsive maneuvers (except, perhaps, those needed for guidance purposes), $V_{\infty_1} = V_{\infty_2}$. The trajectory plane is inclined at angle i to the ecliptic with the line of nodes being the Sun-Jupiter radius vector. The illustration also indicates the general case in which the line of apsides of the post-encounter trajectory is distinct from the line of nodes.

RESULTS

The results are shown in figures 3-9 as contours of selected parameters of the post-encounter trajectories plotted against inclination and pericenter distance of the passage hyperbola. Each figure corresponds to a particular characteristic velocity. For clarity of presentation, each figure is in four parts and contains the following information concerning the post-encounter trajectories:

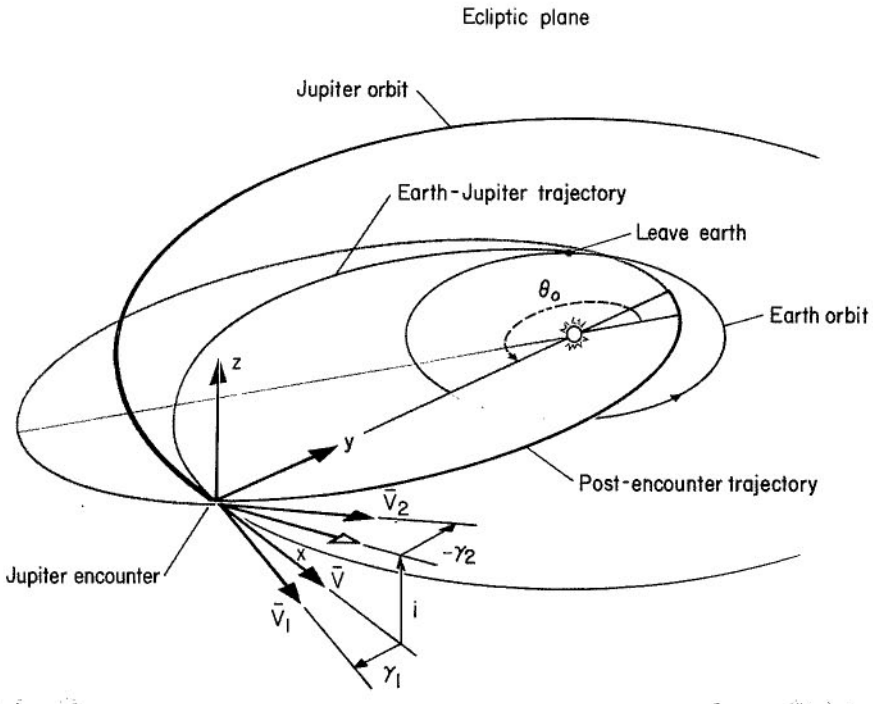

Figure 2.- Jupiter swingby mode out-of-ecliptic/solar probe mission profile.

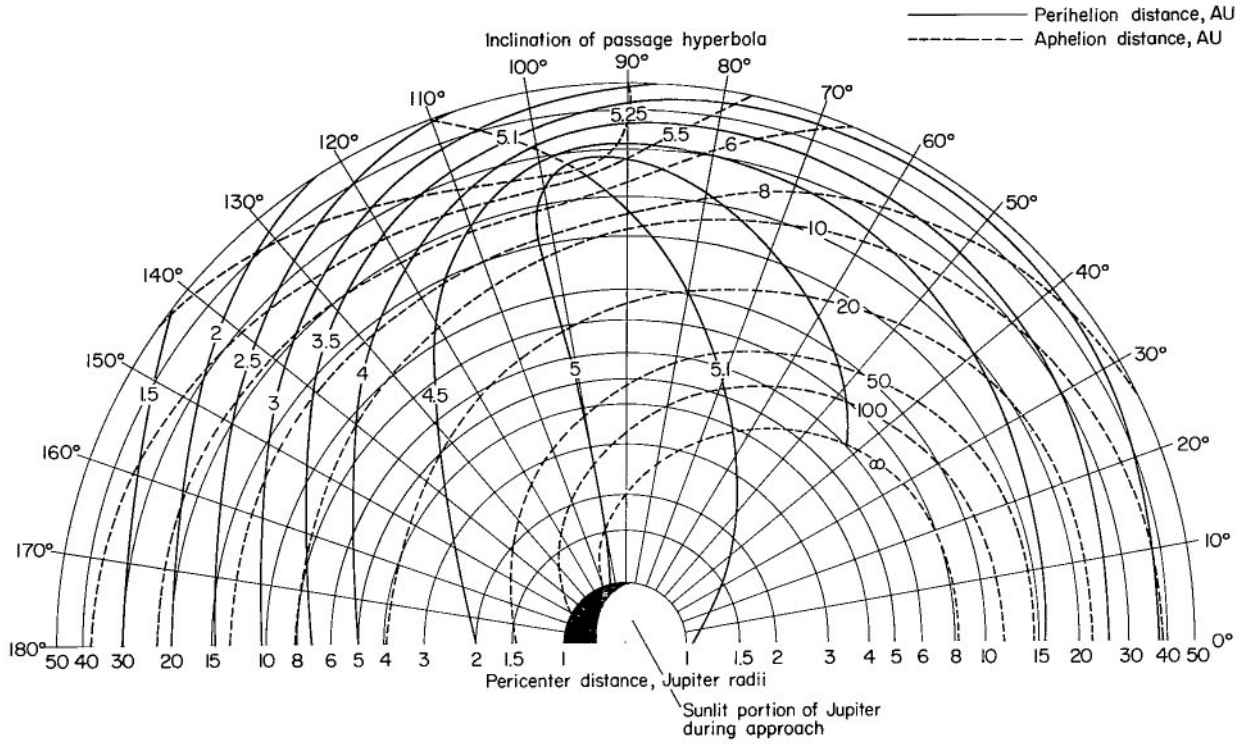

(a) Perihelion and aphelion distances.

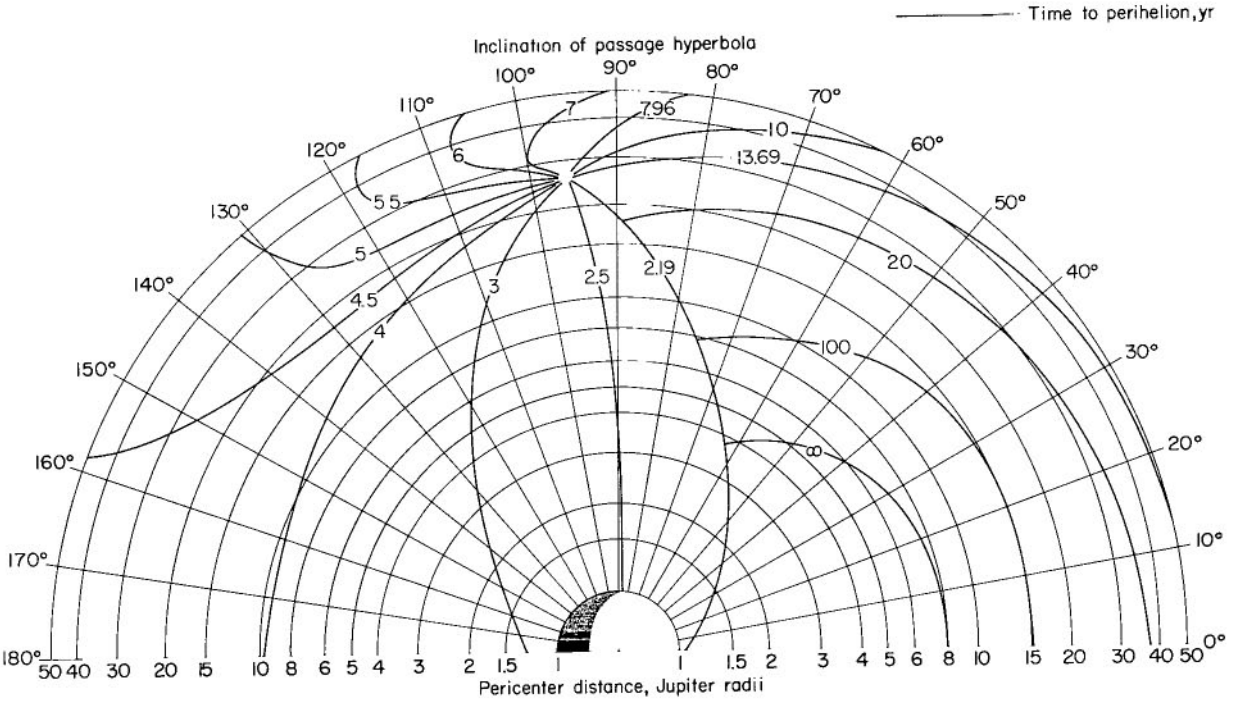

(b) Time to perihelion.

Figure 3.- Post-encounter heliocentric trajectories; V_c = 14.25 km/sec.

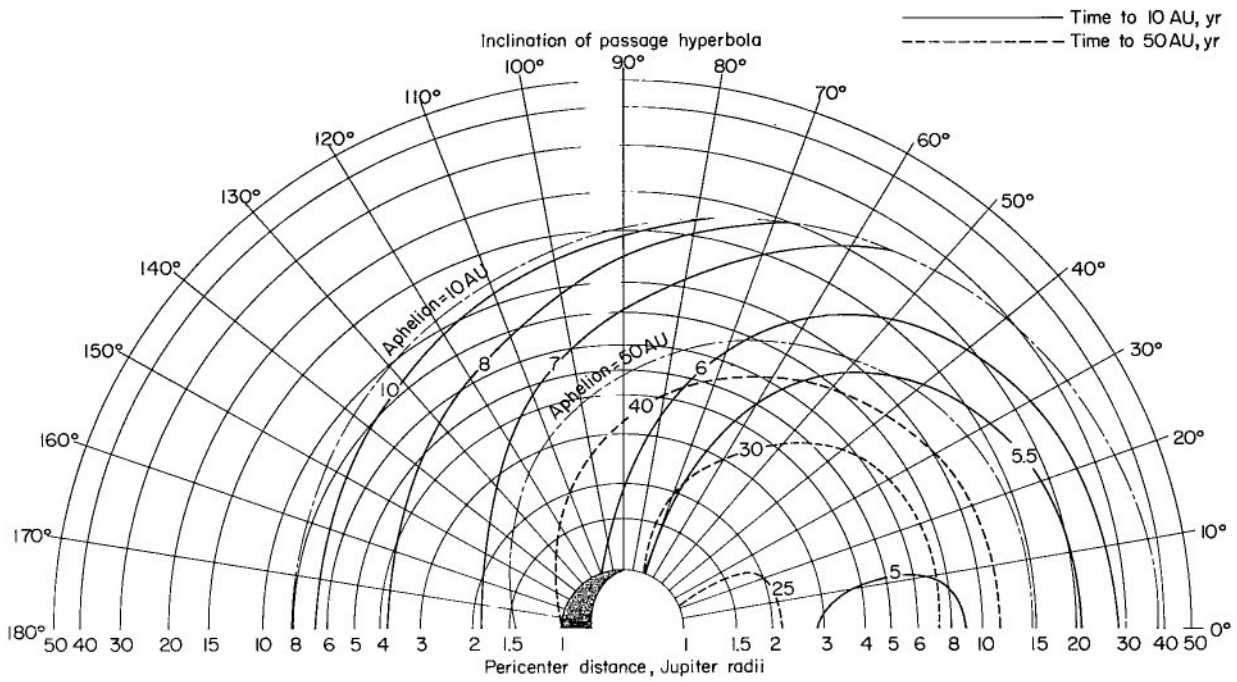

(c) Times to 10 and 50 AU.

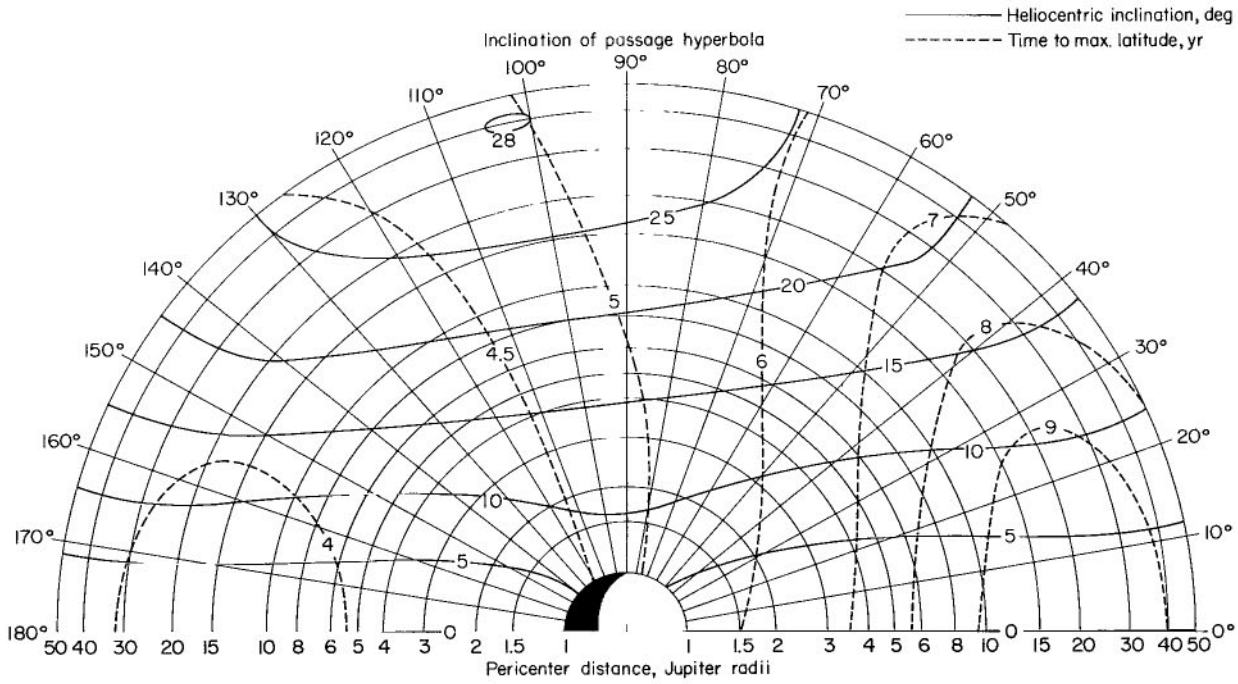

(d) Heliocentric inclination and time to maximum heliocentric latitude.

Figure 3.- Concluded.

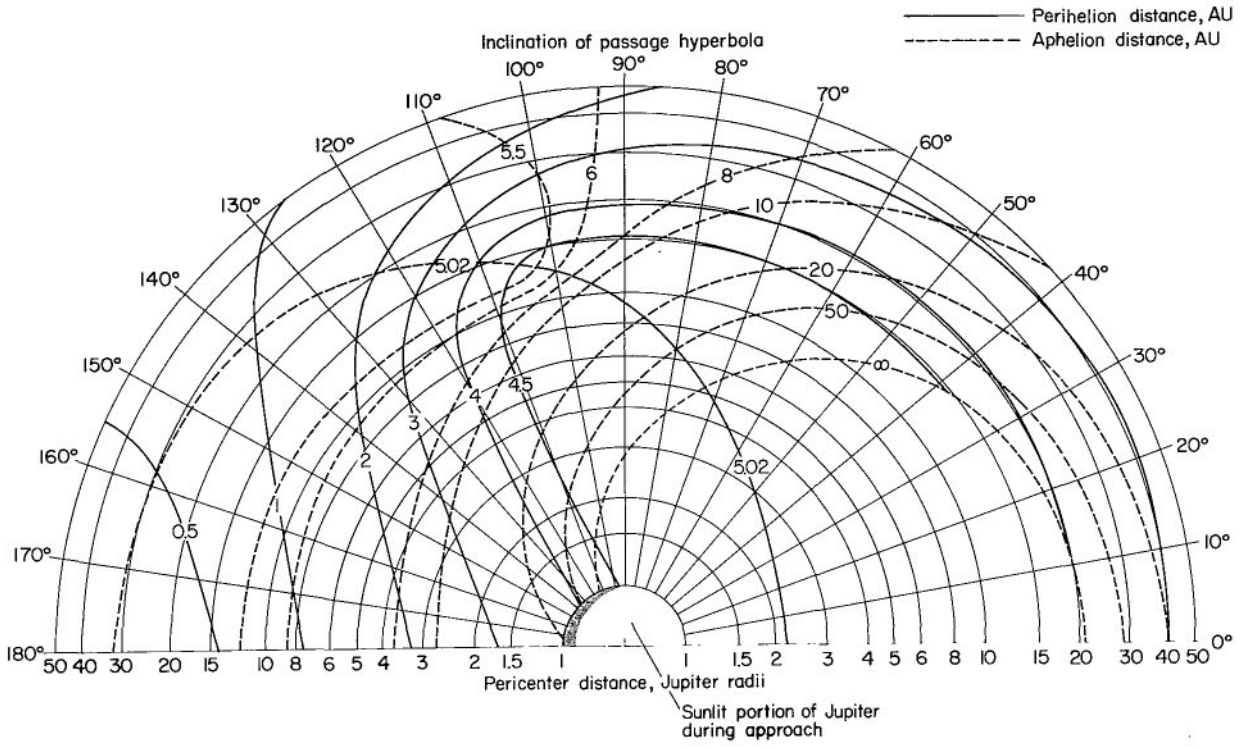

(a) Perihelion and aphelion distances.

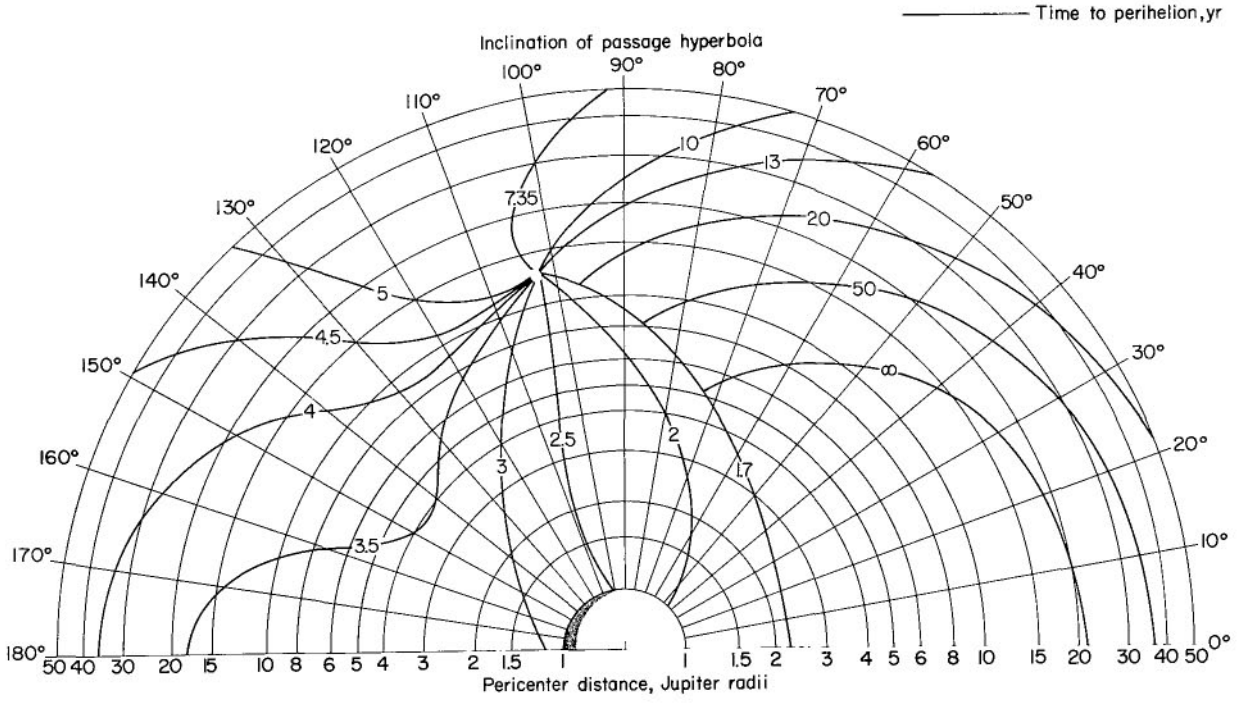

(b) Time to perihelion.

Figure 4.- Post-encounter heliocentric trajectories; V_c = 14.5 km/sec.

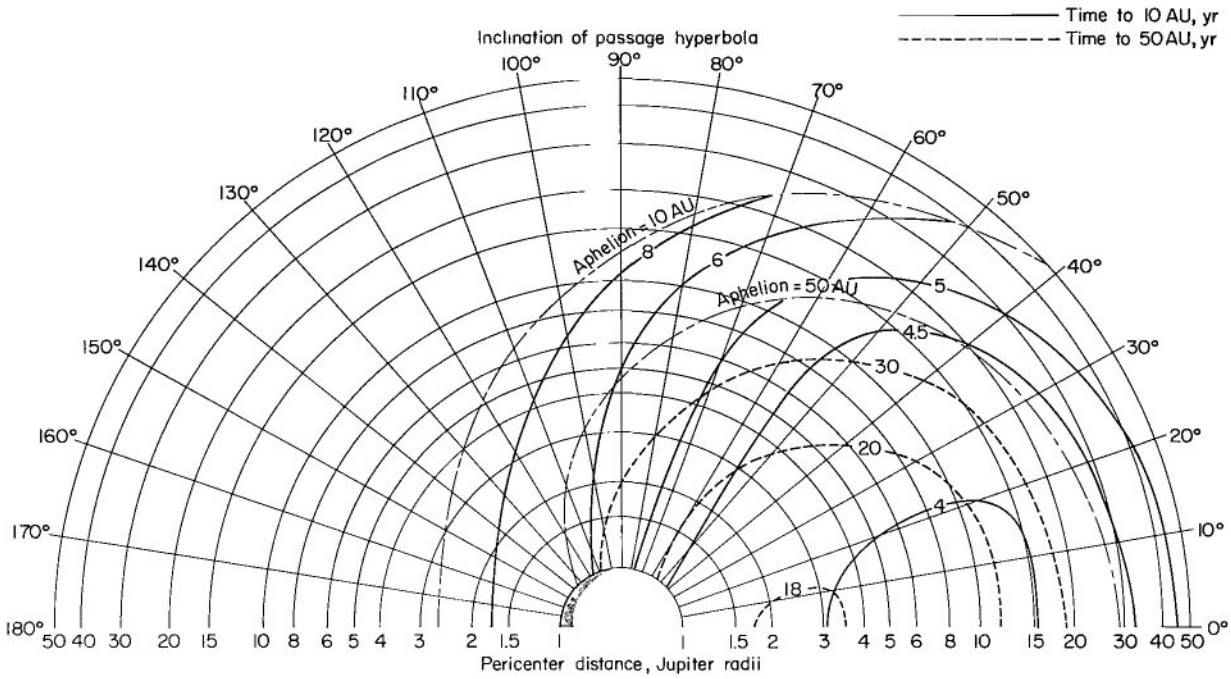

(c) Times to 10 and 50 AU.

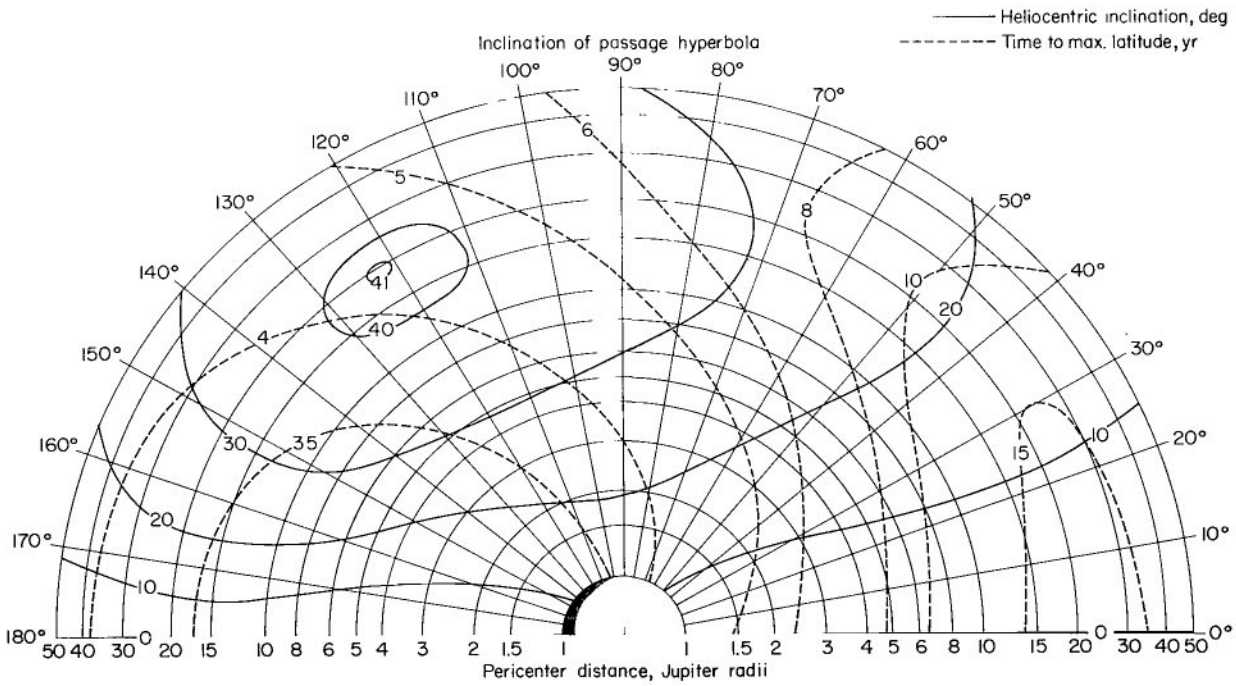

(d) Heliocentric inclination and time to maximum heliocentric latitude.

Figure 4.- Concluded.

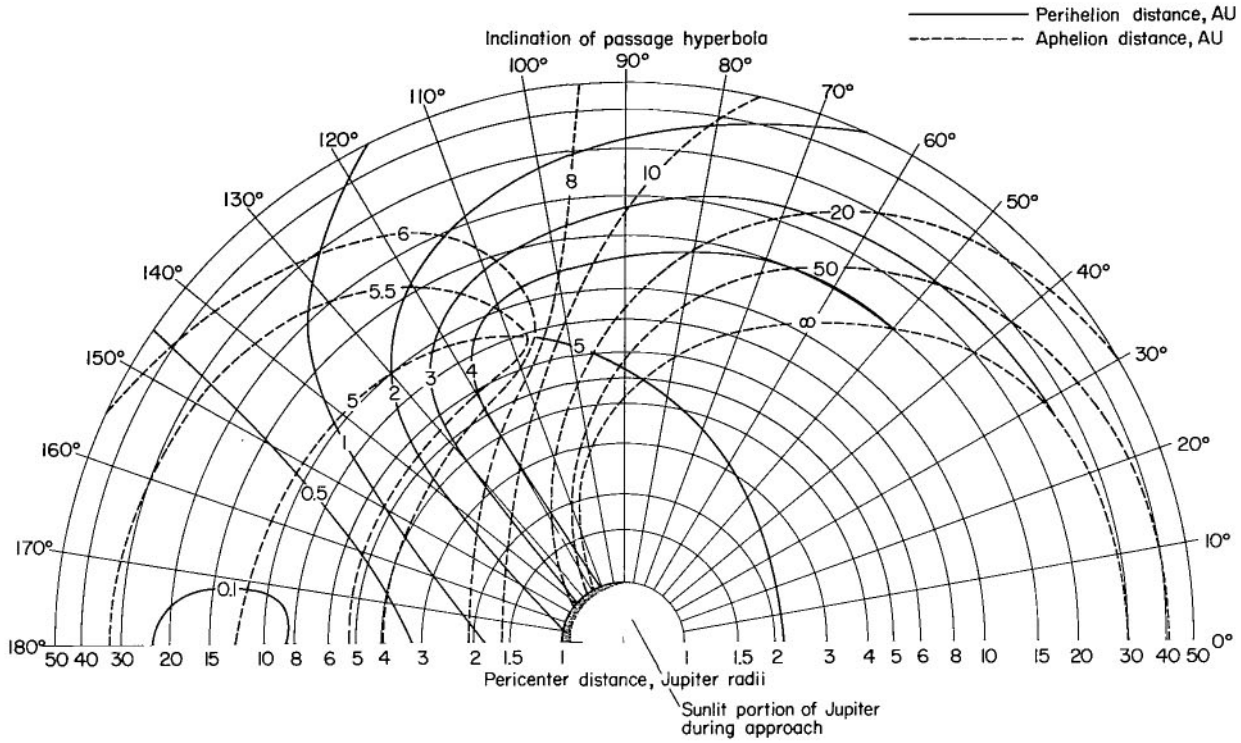

(a) Perihelion and aphelion distances.

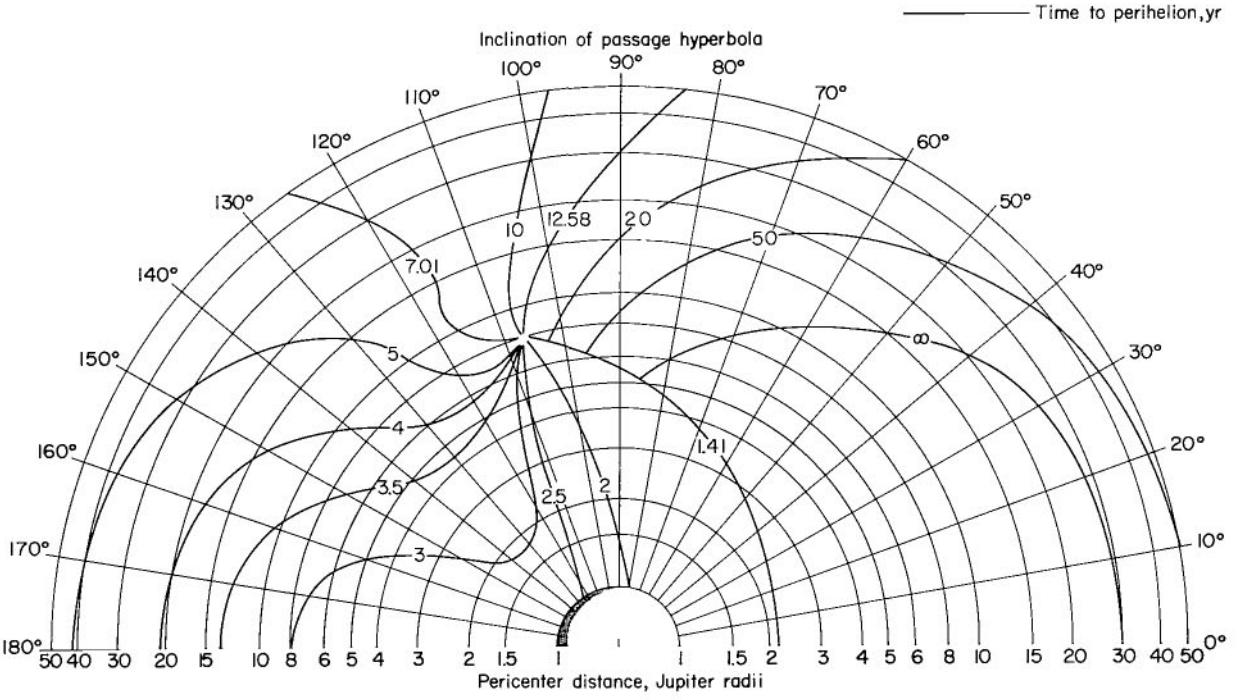

(b) Time to perihelion.

Figure 5.- Post-encounter heliocentric trajectories; V_c = 15 km/sec.

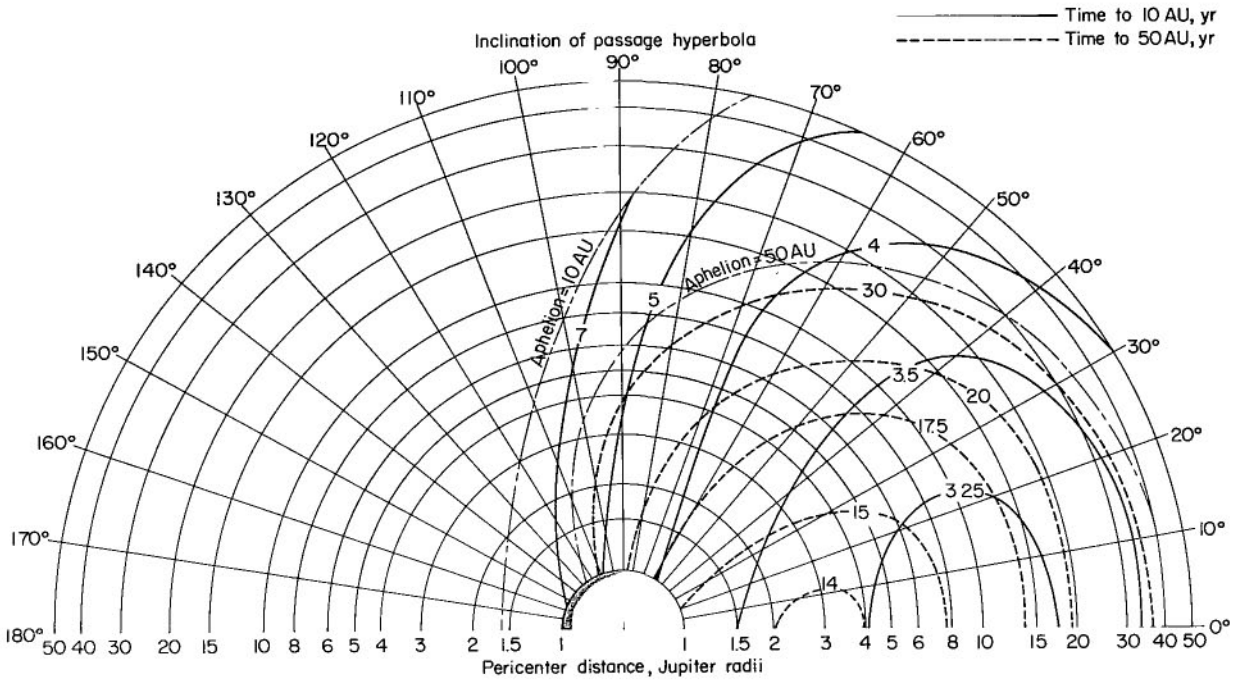

(c) Times to 10 and 50 AU.

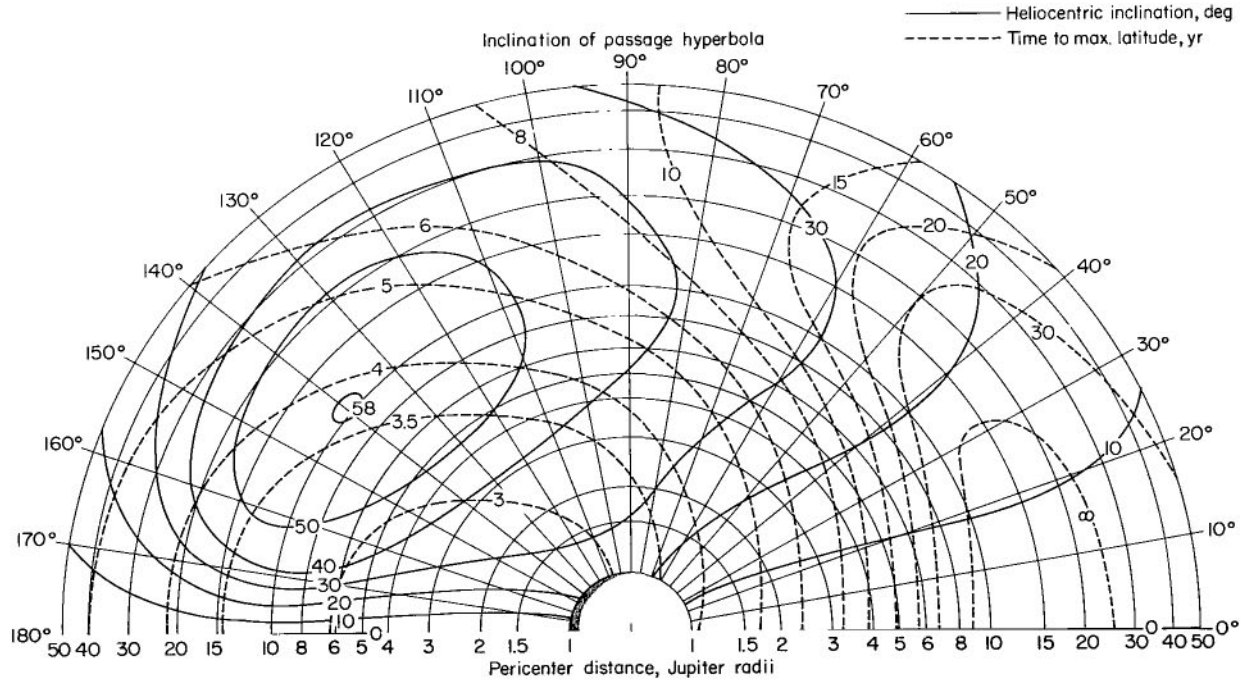

(d) Heliocentric inclination and time to maximum heliocentric latitude.

Figure 5.- Concluded.

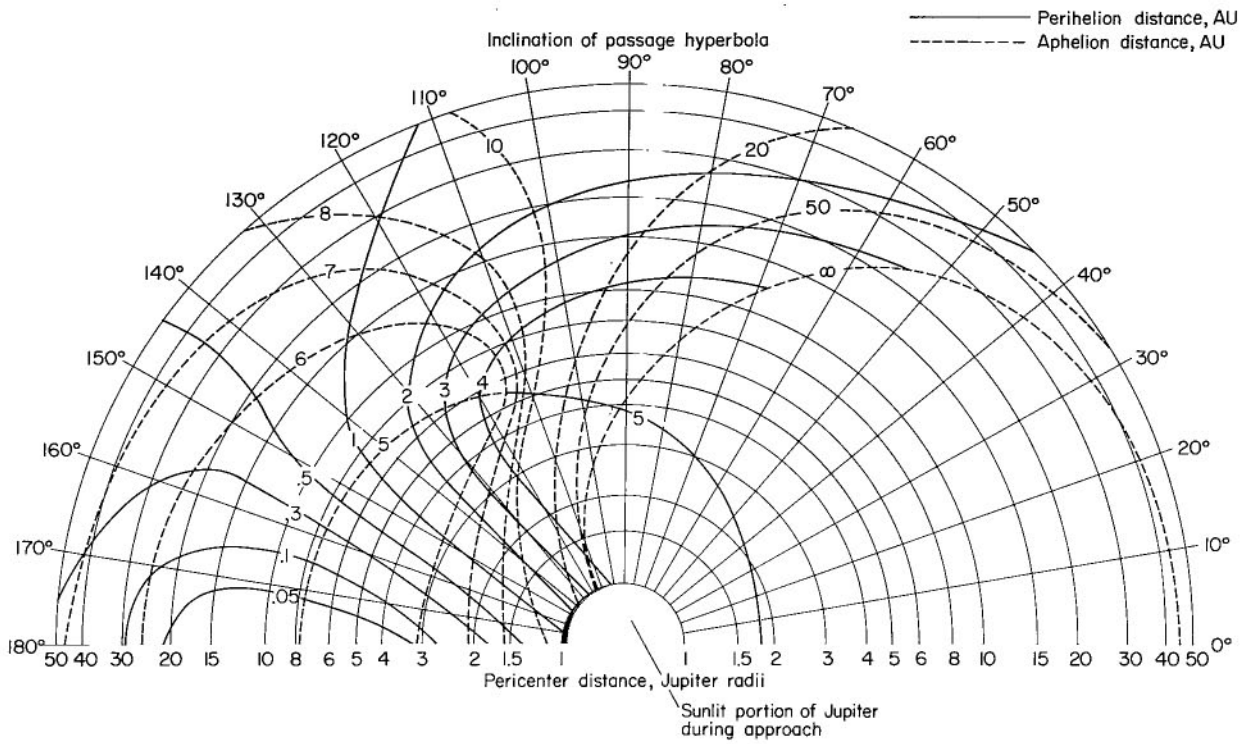

(a) Perihelion and aphelion distances.

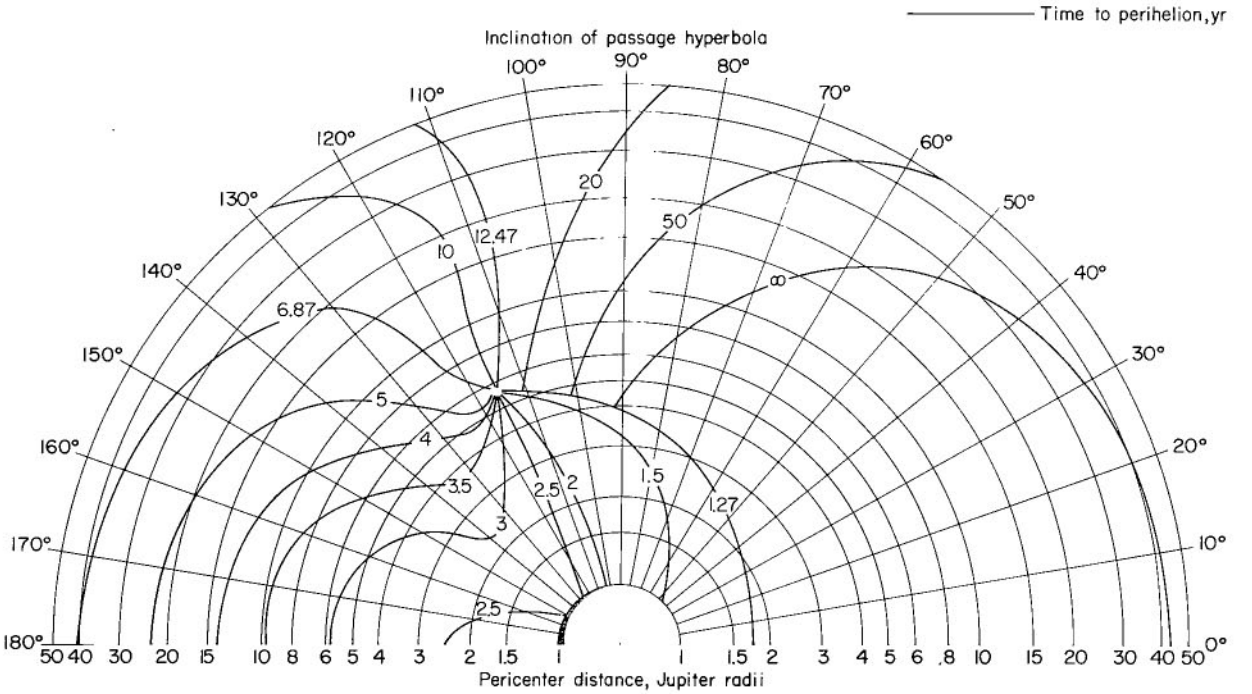

(b) Time to perihelion.

Figure 6.- Post-encounter heliocentric trajectories; V_c = 15.5 km/sec.

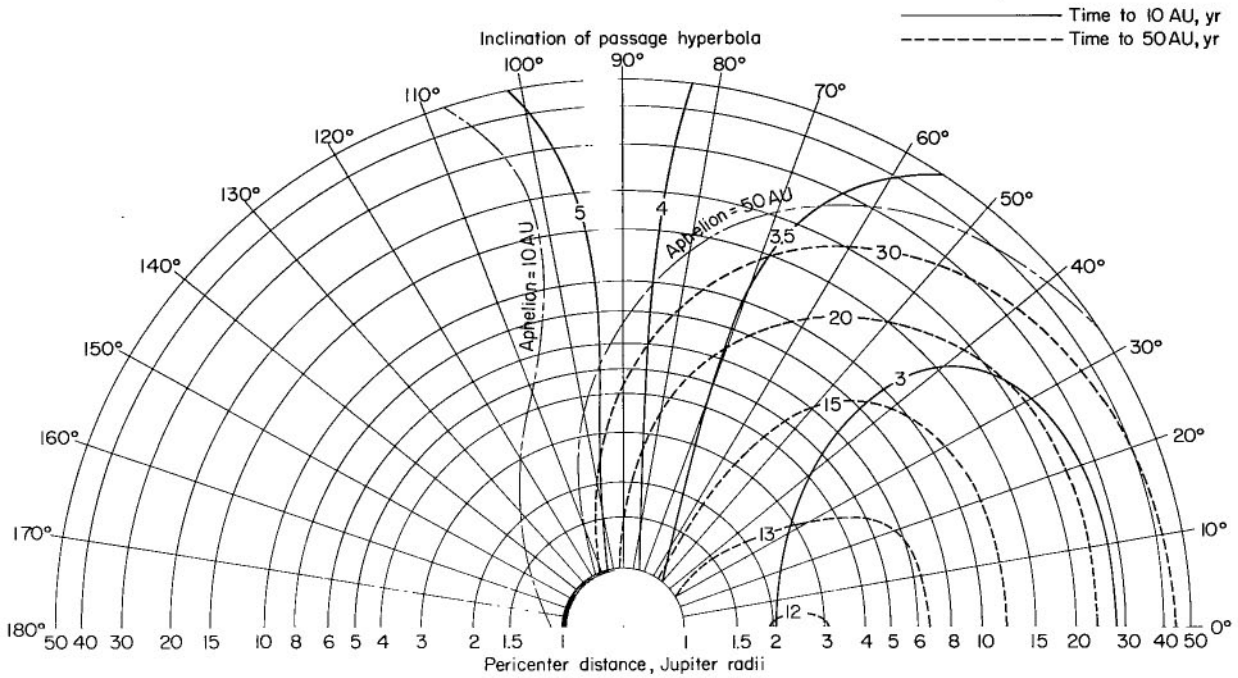

(c) Times to 10 and 50 AU.

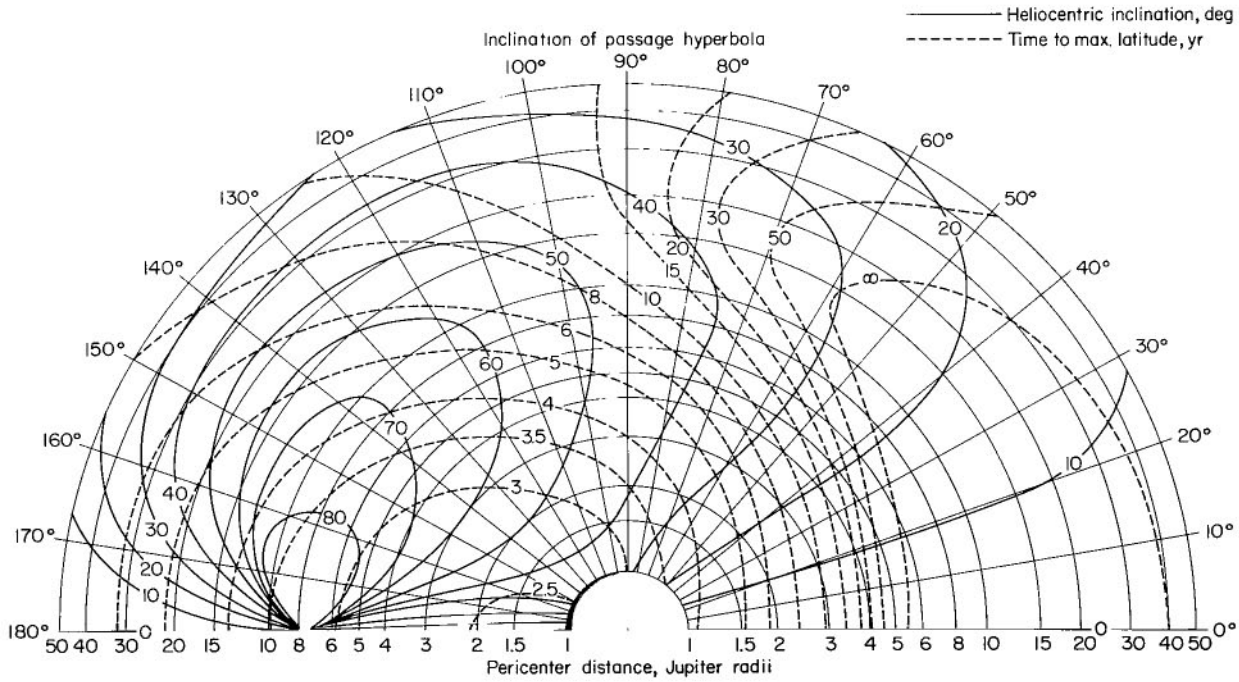

(d) Heliocentric inclination and time to maximum heliocentric latitude.

Figure 6.- Concluded.

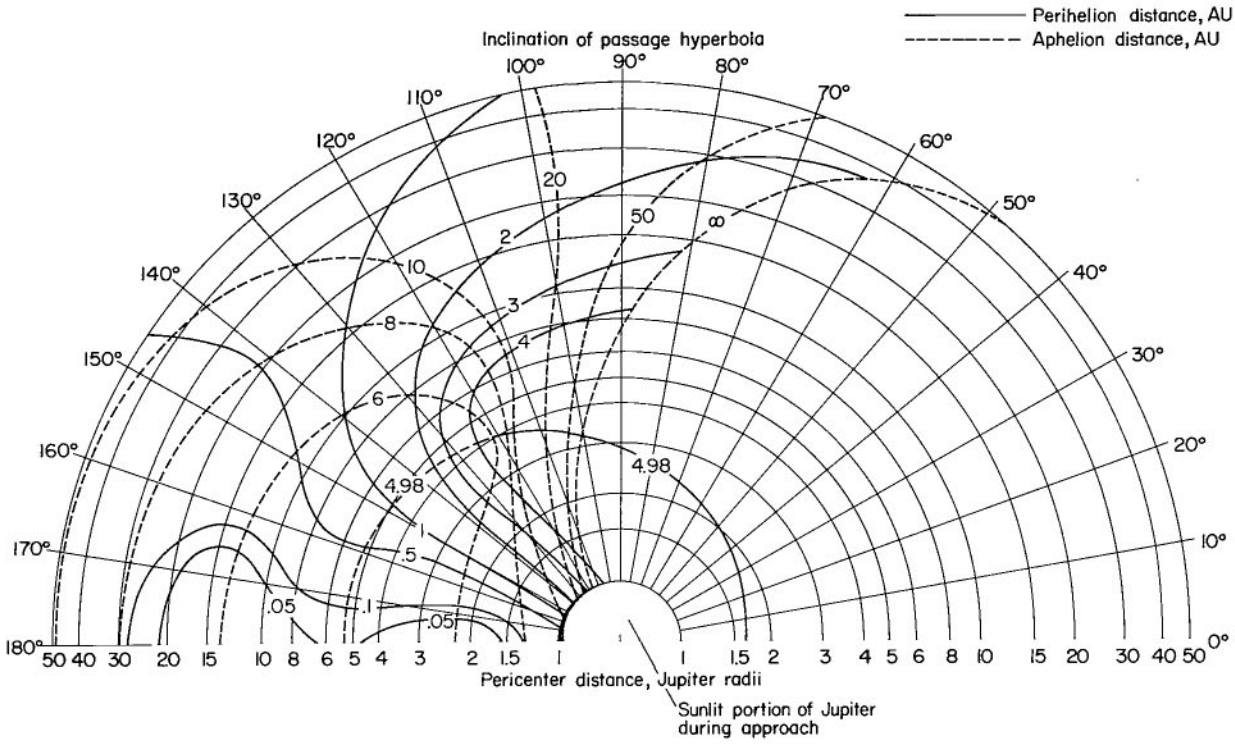

(a) Perihelion and aphelion distances.

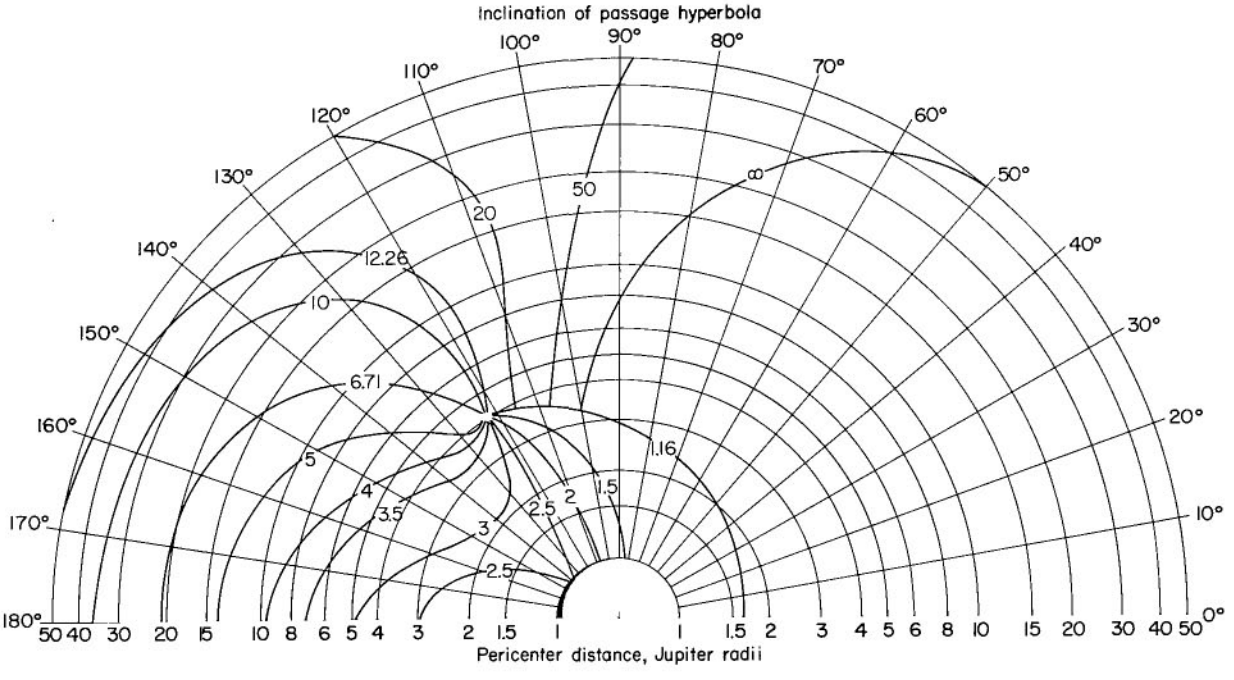

(b) Time to perihelion.

Figure 7.- Post-encounter heliocentric trajectories; V_c = 16 km/sec.

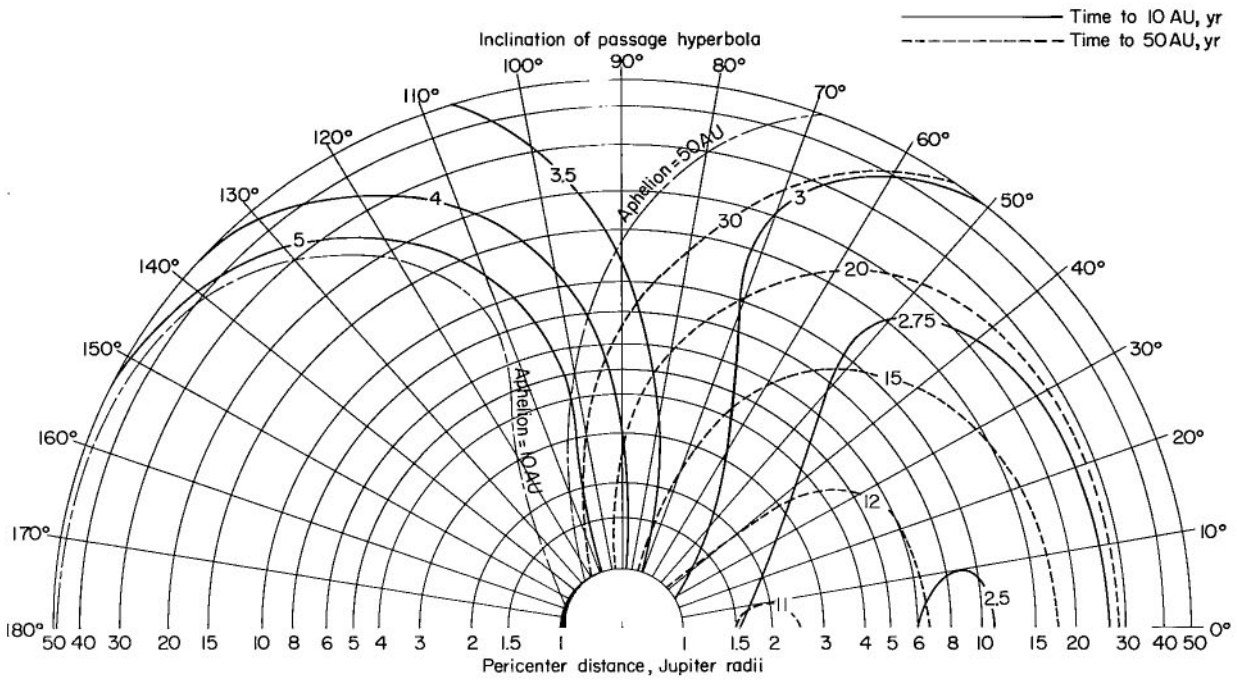

(c) Times to 10 and 50 AU.

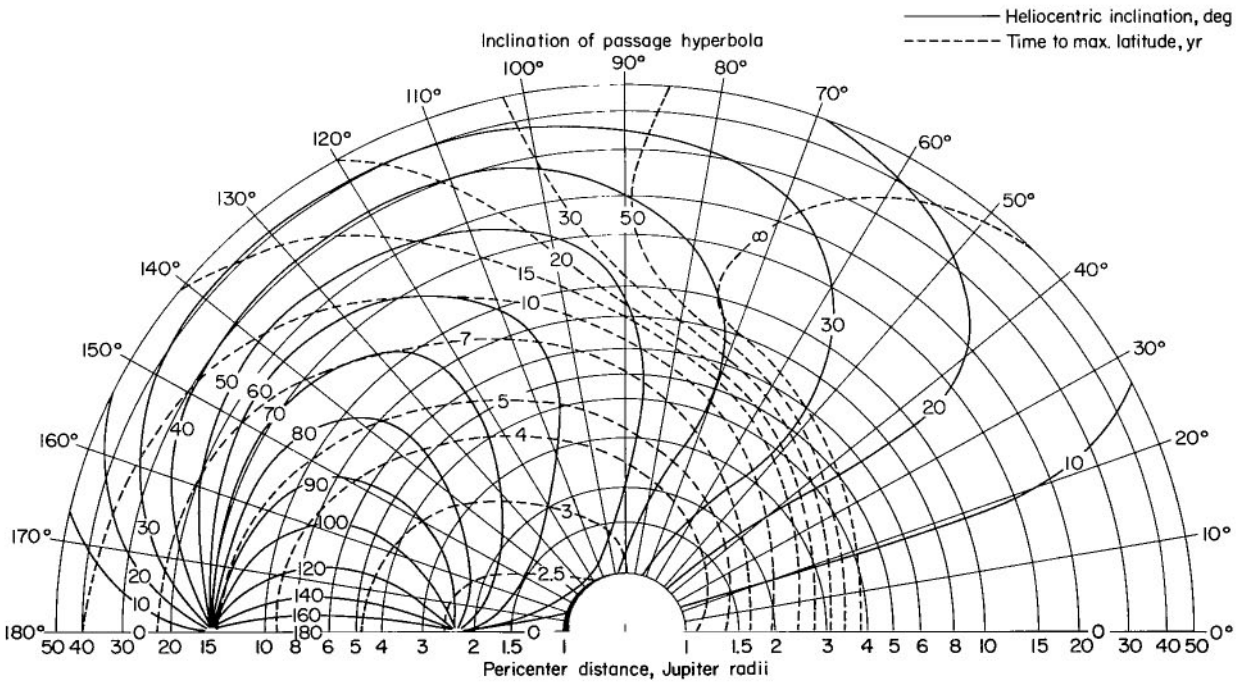

(d) Heliocentric inclination and time to maximum heliocentric latitude.

Figure 7.- Concluded.

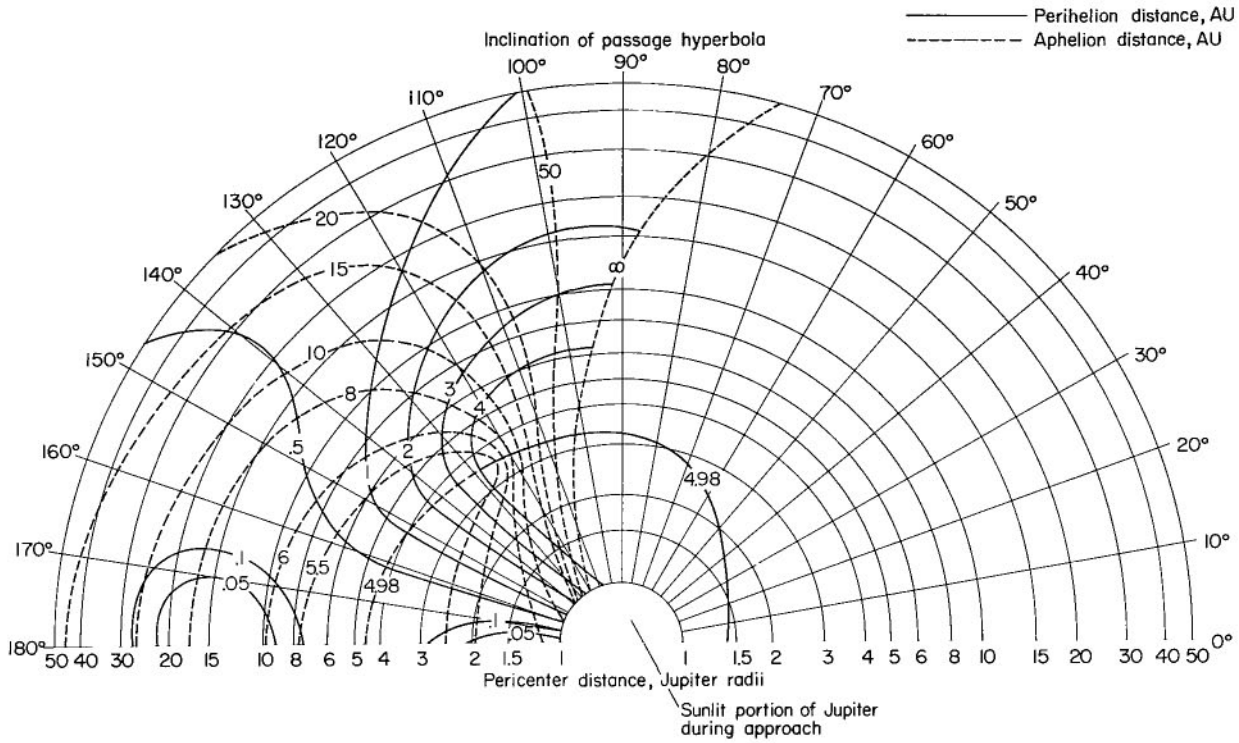

(a) Perihelion and aphelion distances.

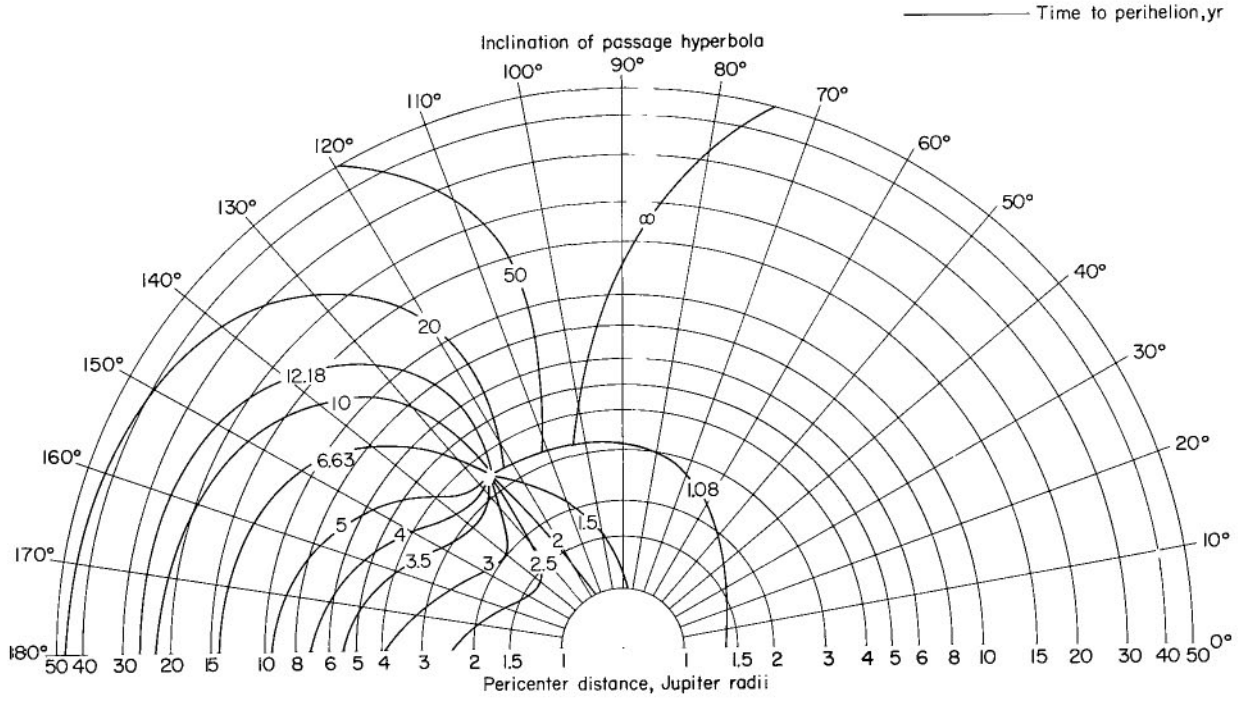

(b) Time to perihelion.

Figure 8.- Post-encounter heliocentric trajectories; V_c = 16.5 km/sec.

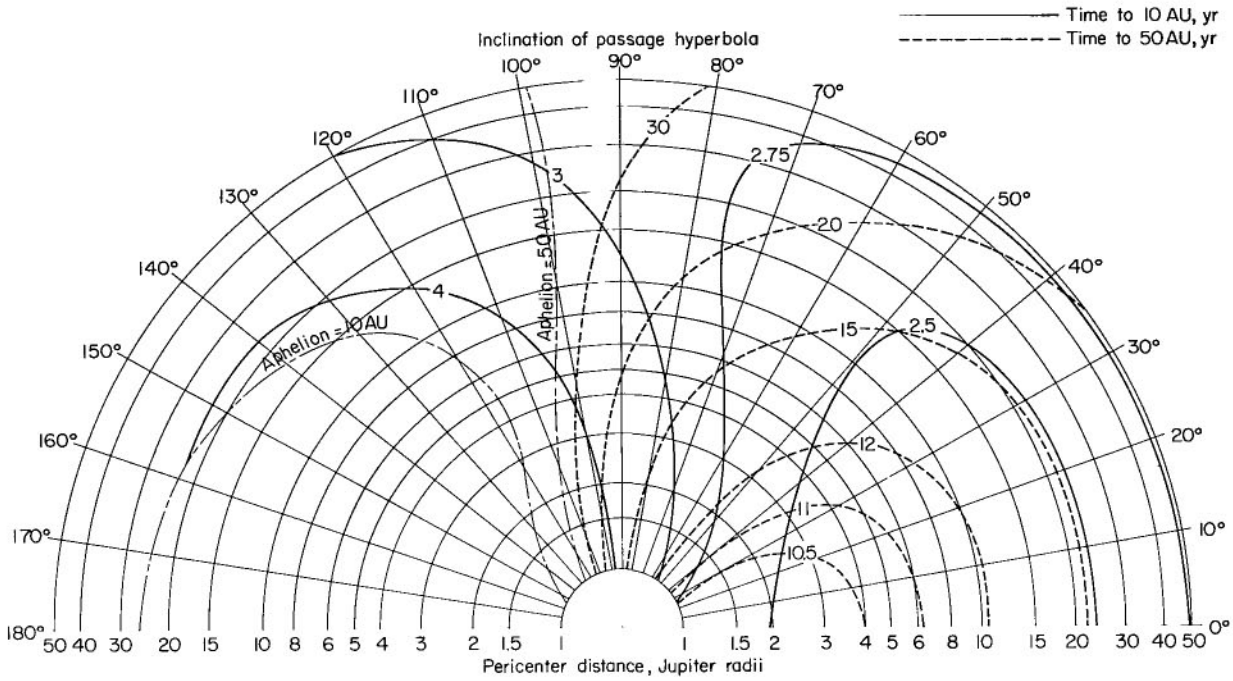

(c) Times to 10 and 50 AU.

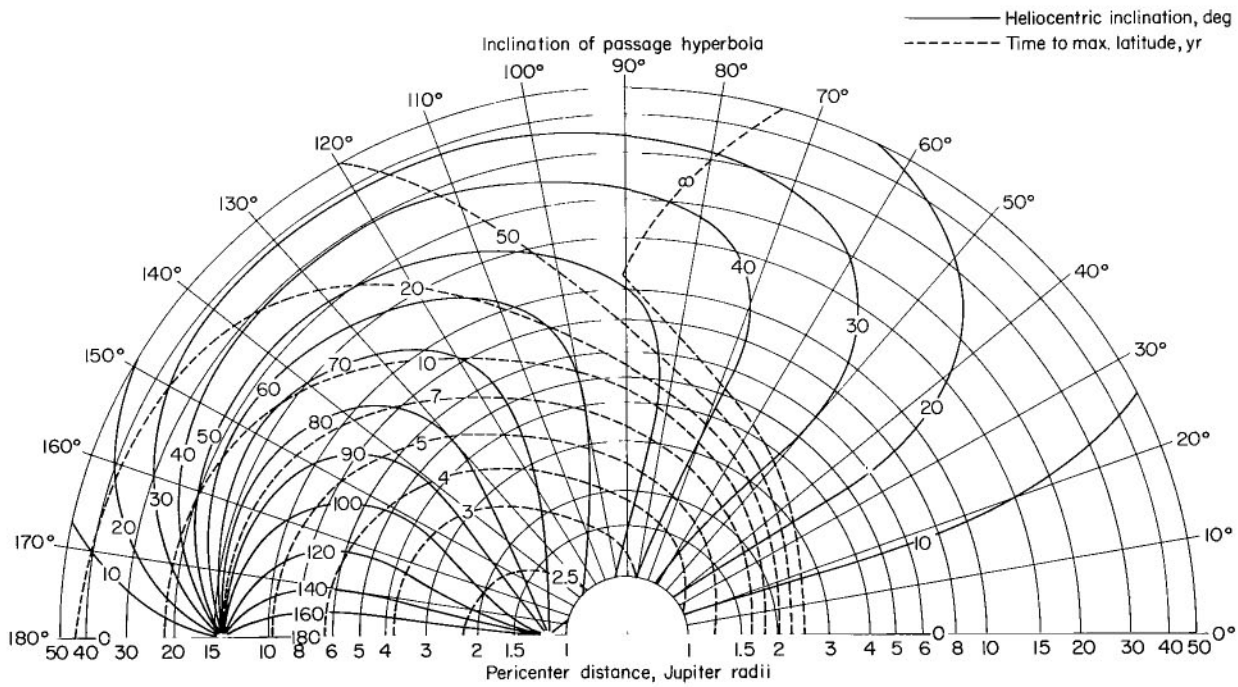

(d) Heliocentric inclination and time to maximum heliocentric latitude.

Figure 8.- Concluded.

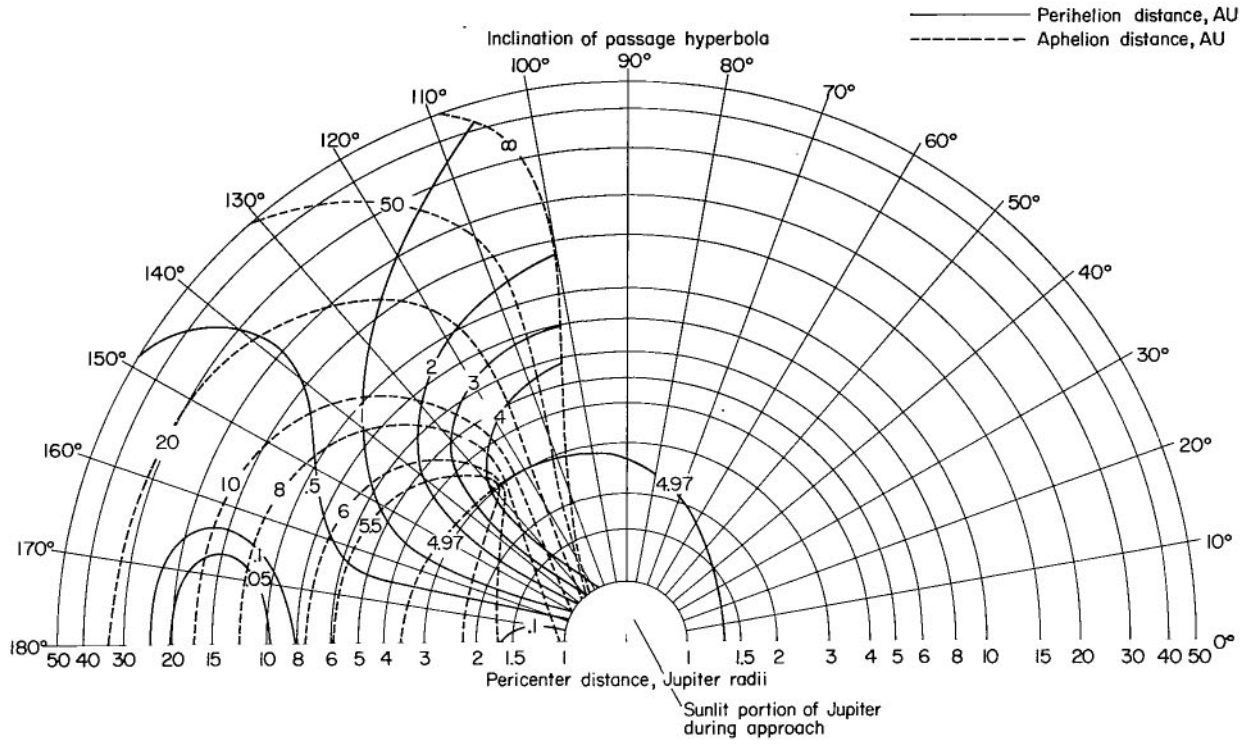

(a) Perihelion and aphelion distances.

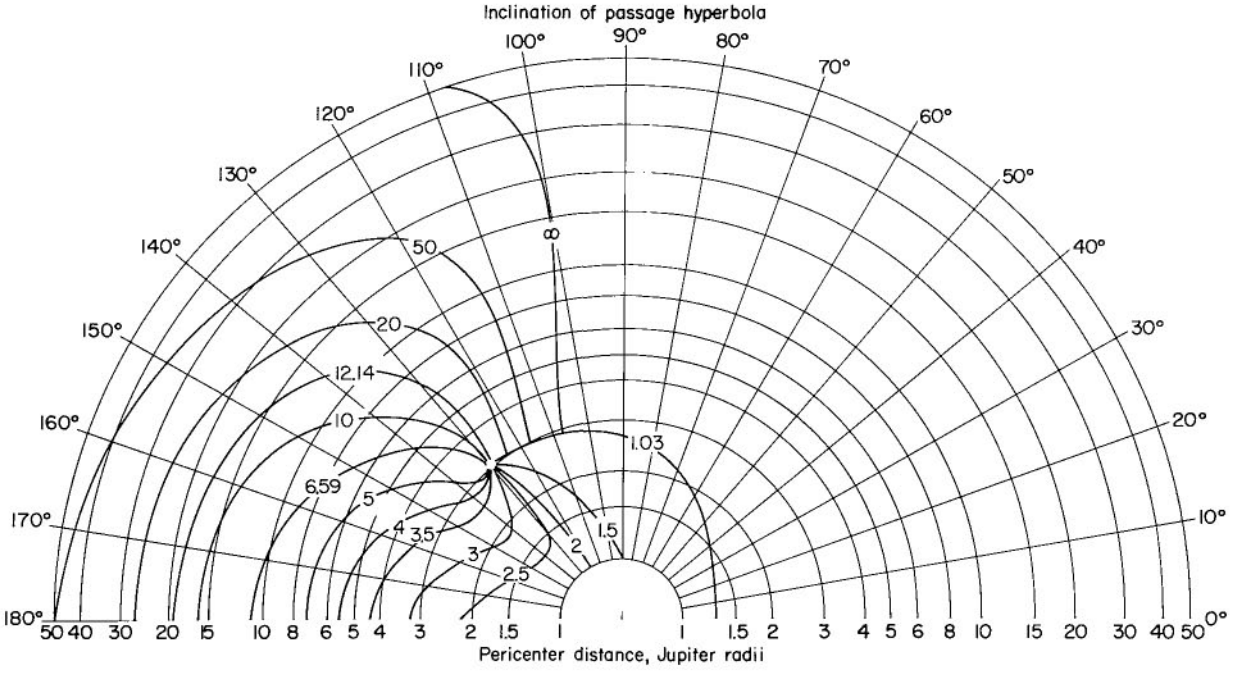

(b) Time to perihelion.

Figure 9.- Post-encounter heliocentric trajectories; V_c = 17 km/sec.

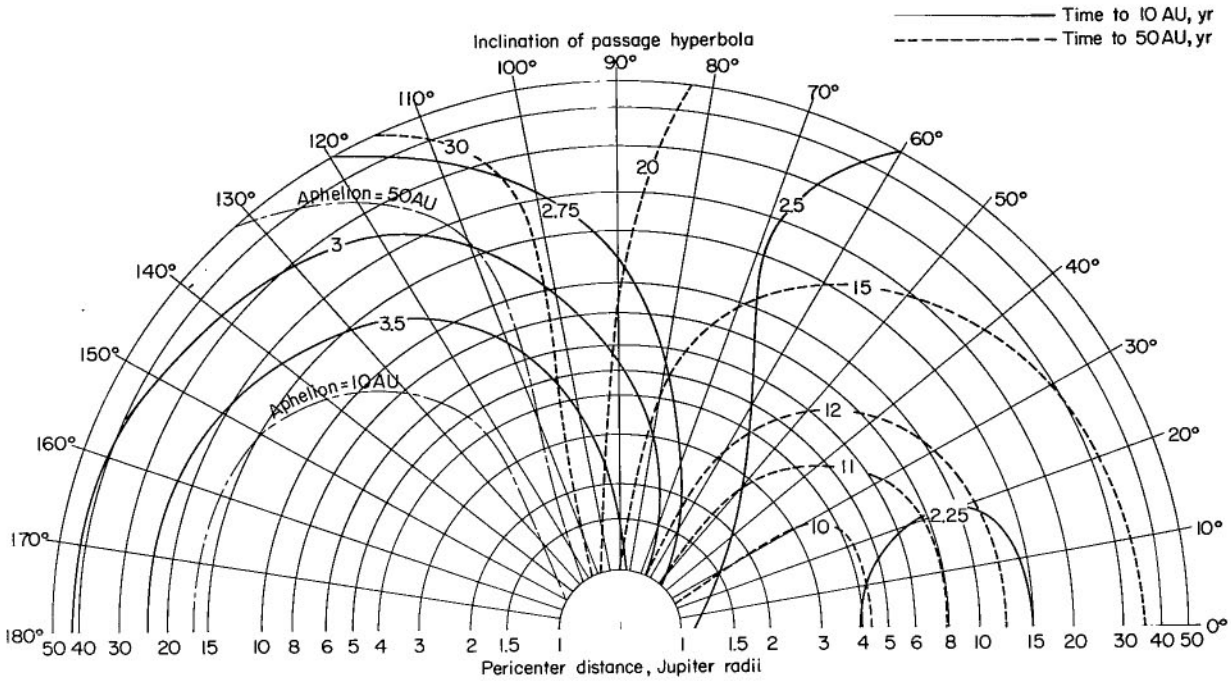

(c) Times to 10 and 50 AU.

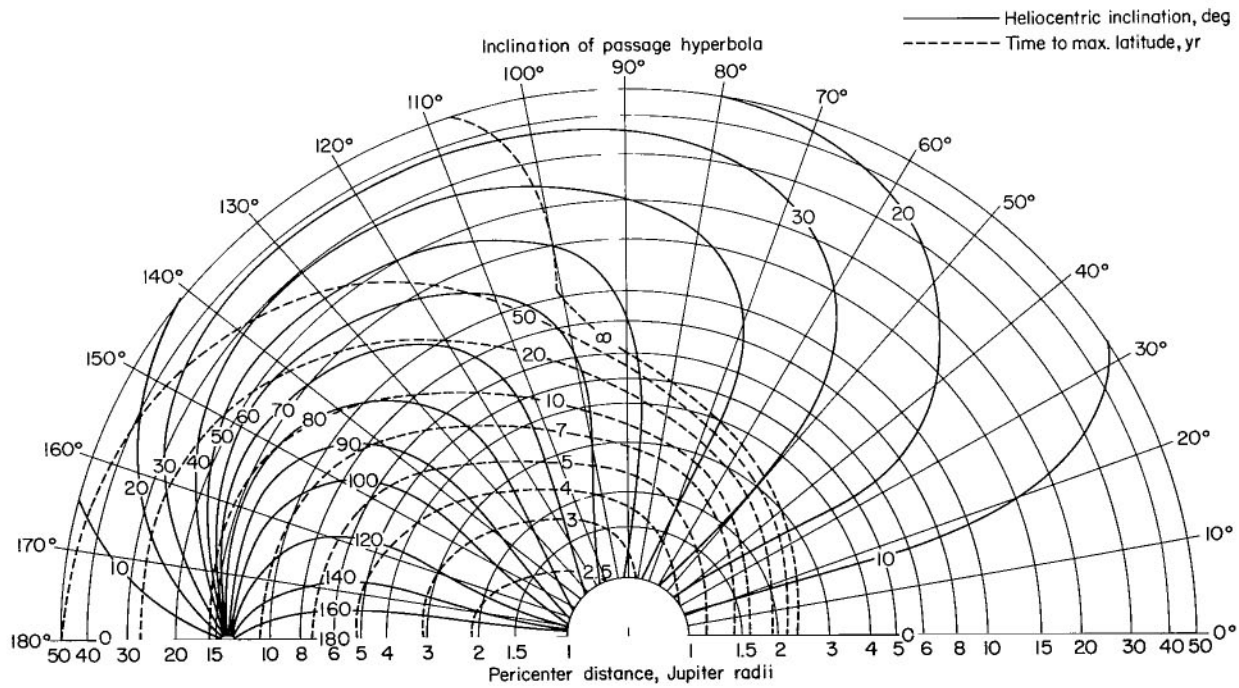

(d) Heliocentric inclination and time to maximum heliocentric latitude.

Figure 9.- Concluded.

Part A, Perihelion and Aphelion Distances - These parameters are of obvious interest for solar probe missions; missions to explore the asteroid belt; and, of course, missions for distant solar system exploration.

Part B, Time to Perihelion - This is the time, measured from Earth departure, until perihelion of the post-encounter trajectory is first reached. It is important because it establishes the spacecraft lifetime requirements for solar probe missions.

Part C, Times to 10 AU and 50 AU - For missions to the distant regions of the solar system, the spacecraft lifetime requirements are even more critical. Unlike mission operation near perihelion (where the rate of change of true anomaly with time, $d\theta/dt$, is large), as a spacecraft approaches aphelion $d\theta/dt$ becomes very small. Consequently, if it were desired to send a spacecraft to a specified large distance from the Sun and if this distance corresponded to aphelion of the post-encounter trajectory, excessive flight times could result. A more reasonable alternative would be to select a trajectory whose aphelion distance is substantially larger than the desired distance. This would include, of course, hyperbolic trajectories for which aphelion is undefined. To illustrate this approach, two distances (10 AU and 50 AU) were selected. The times required to attain these distances are shown for trajectories whose aphelion distances exceed these values.

Part D, Heliocentric Inclination and Time to Maximum Heliocentric Latitude - Heliocentric inclination is a major criterion for estimating the effectiveness of out-of-ecliptic missions. The heliocentric latitude will be less than the inclination, however, except when the true anomaly after encounter is $\pi/2 + n\pi$ ($n = 0, 1, 2, \ldots$), at which points the latitude will assume the value of the inclination. Thus, it seems prudent to specify a spacecraft lifetime sufficient to permit this latitude to be reached. These required times are shown for $n = 0$.

Although the trajectory dynamics, of course, are not dependent on characteristic velocity, the appearances of the charts are quite dissimilar when different velocities are compared. In the following paragraphs, the post-encounter trajectories for each velocity will be discussed individually. Particular attention will be paid to the first set of charts (fig. 3) since they do embody all the features of the swingby mode.

Characteristic Velocity = 14.25 km/sec

The hyperbolic excess velocity vector, $\overline{V}_{\infty_1}$, approaches Jupiter from a direction generally opposed to its orbital motion and somewhat from the direction of the Sun. Consequently, about three-fourths of the planet's disc is visible during the approach phase as shown in figure 3(a).

Consider now the perihelion and aphelion contours labeled 5.1, referred to collectively hereafter as the basic contour. Jupiter's orbital radius at the time of encounter is 5.1 AU. Thus, this curve represents the locus of post-encounter trajectories with one apse at Jupiter (i.e., $Y_2 = 0$). If the passage hyperbolas are chosen along this contour and are such that pericenter distances are less than about 27 radii and inclinations are less than about 96°, the heliocentric speed after encounter, V_2, will exceed Jupiter's orbital speed, V; hence, the spacecraft will emerge from the sphere of influence at perihelion of the post-encounter trajectory. The post-encounter trajectory of maximum heliocentric energy has 0° inclination and has the spacecraft at perihelion immediately after encounter. For this V_c the corresponding pericenter distance is about 1.1 Jupiter radii.

If the pericenter distance and inclination exceed the quoted values, then $V_2 < V$, and the spacecraft will enter the post-encounter trajectory at aphelion. At the singular point $V_2 = V$, and the post-encounter trajectory becomes a circular orbit with radius equal to that of Jupiter at the time of encounter although, as will be seen shortly, substantially inclined to the ecliptic. To the left of the basic contour $Y_2 < 0$; thus perihelion will be encountered before aphelion. To the right of this contour $Y_2 > 0$ and aphelion will be encountered first.

Post-encounter trajectories that result from passage hyperbolas with low inclinations (the right portion of the chart) will realize a positive energy transfer from Jupiter's gravitational field. An energy loss will result when the inclinations are very high (i.e., retrograde with respect to Jupiter). To a certain extent this is shown by comparing the perihelion radii between the left and right portions of the chart. For a given passage distance, the perihelion radii associated with the retrograde passages are uniformly less. Notice that, regardless of passage inclination, the perihelion distance varies inversely with passage distance. For very large passage distances, the perihelion distance will approach 1 AU. This is the value that would be associated with the post-Jupiter phase of the unperturbed Earth-Jupiter trajectory. Since the perihelion distances are never less than 1 AU, it is obvious that this (minimum energy) Jupiter swingby is not compatible with solar probe missions.

Examination of the aphelion contours reveals more evidence of the energy transfers that are possible. The curve labeled ∞ is the locus of parabolic post-encounter trajectories. All trajectories contained within this boundary are heliocentric hyperbolas. Thus, this lowest energy Earth-Jupiter trajectory can provide a capability for more distant solar system exploration. As seen, aphelion distance also varies inversely with passage distance. Note, however, the difference in curvature between the 5.25-AU and 5.5-AU contours. Aphelion distance of the unperturbed trajectory is 5.25 AU. Thus, this contour "folds back" and, for large passage distances, would circumscribe the entire chart.

As a final observation of figure 3(a), note that the right portion of the 5-AU perihelion contour does not penetrate into the region of hyperbolic trajectories. Recall that to the right of the basic contour $Y_2 > 0$. Thus,

within the hyperbolic region to the right of the basic contour, the spacecraft enters the post-encounter trajectory past perihelion and, of course, never returns.

Turning now to figure 3(b), note first the singularity that exists in time to perihelion at the point that corresponds to the circular post-encounter orbit. Beginning with the 2.19-year contour, this is simply the transfer time from Earth to Jupiter and is equivalent to the $\gamma_2 = 0$ contour discussed above. This is so because, by definition, the time from encounter to perihelion is zero along this contour. At the other extreme, consider the 13.69-year contour. This is the sum of the period of a circular orbit at 5.1 AU and the Earth-Jupiter transfer time. This represents a time to perihelion at the point of singularity, since any positive γ_2, however small, requires that one complete orbit must be completed before perihelion is reached. The third noninteger contour (7.96 year) is that for which the time to perihelion is the sum of the Earth-Jupiter transfer time and one-half the circular orbit period. This is also contained at the singular point since for $V_2 < V$ by an arbitrarily small value, perihelion will be reached one-half period later. It should now be apparent that all contours of time to perihelion not greater than the time to complete one circular orbit converge to the singularity simply because the location of perihelion of a circular orbit is not defined.

For times greater than this value, discontinuous contours also exist as seen from the figure. For example, the 20-year contour is continuous only to the right of the basic contour. At its intersection with the basic contour, the time to perihelion is double valued. Thus, perihelion can occur either immediately after emergence from the sphere of influence ($\gamma_2 \rightarrow 0$ from a negative value) or, for arbitrarily small $\gamma_2 > 0$, will occur after one complete elliptical orbit has been completed. Moving down the chart (toward trajectories of higher energy) the time to perihelion increases until parabolic orbits are attained.

Finally as will be more apparent when higher values of V_c are discussed, the time contours fold back at larger passage distances as do the aphelion distance contours. The time to perihelion of the unperturbed ellipse is about 5.6 years.

The contours of constant flight times to 10 AU and 50 AU are shown in figure 3(c). The 10 AU and 50 AU aphelion contours from figure 3(a) are also shown since they bound the region of applicability of this chart. The times to aphelion vary, of course, along these aphelion contours.

It is seen first that the minimum time to travel to 10 AU is slightly less than 5 years; the maximum times can exceed 10 years. Referring again to figure 3(a), note that for the minimum transfer time $\gamma_2 > 0$. In other words, some energy is sacrificed to increase the radial velocity component of the post-encounter trajectory. This is appropriate only because the ratio of final to initial radius is small (~2). As this ratio increases, it becomes more important to increase energy in order to reduce the flight time. This is apparent by examination of the time contours associated with flights to 50 AU;

the minimum time contour of 25 years is centered about the $\gamma_2 = 0$ contour. Because of this long flight time, one concludes that this minimum energy mission to Jupiter is inappropriate for use with post-encounter missions whose purpose is exploration at the fringe of the solar system.

As the characteristic velocity is increased, the minimum times to perihelion or to a fixed radius tend to decrease in a regular manner. Since no unique features will subsequently present themselves, the associated charts will be mentioned only in passing.

The final chart (fig. 3(d)) concerns the out-of-ecliptic potential for the post-encounter trajectories. Heliocentric inclinations up to 28° are possible with this minimum energy mission. (To attain this inclination with the direct flight mode, a characteristic velocity of almost 18 km/sec would be needed.) If the hyperbolic excess speed is less than Jupiter's orbital speed, the trajectory of maximum inclination has as initial conditions that $\gamma_2 = 0$ and that the spacecraft emerges from the sphere of influence at aphelion. This can be seen by noting the location of the basic contour from figure 3(a).

At least 4 years are required to attain maximum latitude. Such long times result because of the rather large perihelion distances discussed earlier. The constant time contours exhibit the change in curvature, noted previously, between 5 and 6 years. (The time needed to travel through a 90° transfer angle measured from Jupiter on the unperturbed trajectory is slightly more than 5 years.)

Characteristic Velocity = 14.5 km/sec

As characteristic velocity is increased, the hyperbolic excess approach vector rotates toward the Jupiter-Sun line, making more of the planet's disc visible, as seen in figure 4(a). The magnitude of the excess speed also increases (fig. 1) with V_C. For values of V_C below about 15.5 km/sec (for which, $V_\infty = V$), this results in certain well-defined trends that are summarized below (fig. 4(a)-(d)).

The minimum value of V_2 ($V_{2\,min} = V - V_\infty$) becomes less, permitting smaller perihelion radii. From figure 4(a), perihelion radii less than 0.5 AU are possible. Conversely, the maximum value of V_2 ($V_{2\,max} = V + V_\infty$) becomes greater. Hence, the heliocentric energy can also be increased to a greater extent. This is demonstrated by the larger region for which hyperbolic post-encounter trajectories become possible.

The maximum possible heliocentric inclination increases to about 41° (fig. 4(d)). To achieve the maximum inclination, the passage hyperbola becomes more highly inclined and the associated pericenter distance decreases. The variation increases between the minimum and maximum times required to attain maximum latitude. For retrograde passage inclinations, the minimum time is less than 3.5 years. For posigrade passages, however, the maximum time is increased to over 15 years.

Characteristic Velocity = 15 km/sec

At this energy level, trajectories become possible with significant capability to fulfill multiple mission objectives in shorter times. Consider, for example, a passage inclination of about 172° and a pericenter distance of 10 radii. From figure 5, the post-encounter trajectory plane will be inclined 30° to the ecliptic; perihelion distance of this trajectory will be 0.1 AU; and the time required to reach maximum latitude and perihelion will be less than 3.5 years.

A similar spacecraft lifetime will permit observations to be made at 10 AU if the passage hyperbola is chosen accordingly. A peculiar feature of the hyperbolic post-encounter trajectories also arises at this energy level. This is the fact that from figure 5(d), the times required to reach maximum latitude can become infinite. Recall that maximum latitude is reached when the transfer angle after encounter is 90°. When the hyperbola is entered at a significant angular distance past perihelion (i.e., Y_2 large), the transfer angle to the asymptote of this hyperbola becomes less. Eventually, this angle becomes less than 90°, so that maximum latitude (in the sense that maximum latitude equals inclination) is never reached.

Characteristic Velocity = 15.5 km/sec

From figure 1, the excess speed at Jupiter is nearly equal to Jupiter's orbital speed. Thus, since Jupiter's gravitational field remains sufficient to impart the appropriate change in direction to the $\overline{V}_\infty$ vector, the passage conditions can be chosen so that $\overline{V}_2 = 0$. For such a trajectory, the angular momentum is zero and the spacecraft falls into the Sun (fig. 6(a)). This phenomenon exists for purely retrograde passages with a pericenter distance of about 7.7 radii. High values of heliocentric inclination are also possible. All inclination contours converge to this singular point for which inclination is undefined.

Characteristic Velocity = 16 km/sec

At this energy level, the excess speed at Jupiter exceeds Jupiter's orbital speed. Consider again the purely retrograde passages if the pericenter distance is 15 radii (fig. 7(a)). The post-encounter velocity vector will be directed outward from the Sun at an angle $Y_2 = 90°$. As before, the spacecraft will fall into the Sun. As passage distance is decreased (i.e., increased rotation of the excess speed vector) Y_2 exceeds 90°, and the plane of the post-encounter trajectory is inclined 180° to the ecliptic (i.e., the motion is purely retrograde relative to the Sun). This condition exists until a pericenter distance of about 2.4 radii is attained. At this value, the increased rotation of the excess speed vector makes $Y_2 = 270°$. Thus, V_2 is directed toward the Sun and another singularity exists. Further reductions in passage distance cause the heliocentric inclination once again to be zero.

Characteristic Velocity = 16.5 km/sec

The character of these results (fig. 8) is similar to the results just discussed. Note, however, that the singularity that corresponds to $\Upsilon_2 = -90°$ occurs at a much lower radius. This lower value is needed to impart sufficient rotation to the excess speed vector at Jupiter that is increasing monotonically with V_c.

Characteristic Velocity = 17 km/sec

From figure 9(a), note that the second singularity vanishes since the required passage distance is less than 1 radius. But all in all, the features of solar probe or out-of-ecliptic missions have remained quite similar at these higher energy levels.

To illustrate further the energy changes that are possible when Jupiter's gravitational field is used, recall from figure 1 that the Earth-Jupiter trajectory at this characteristic velocity is hyperbolic. Note, however, that for passage inclinations greater than about 100°, all post-encounter trajectories become elliptical.

Lastly, consider the times required for distant solar system exploration; it is seen (fig. 9(d)) that a spacecraft with this characteristic velocity can be made to pass 10 AU in slightly more than 2 years. Exploration at 50 AU can be accomplished if the spacecraft can be made to survive about 10 years. Note that the corresponding time for the unperturbed trajectory would have been between 20 and 30 years.

Effects of Other Launch Years

The variations in Earth-Jupiter trajectory characteristics throughout an 11-year span of launch opportunities were described earlier. A brief investigation of the effects of such variations on the post-encounter trajectories was also conducted for the 1970 and 1980 opportunities. The 1970 opportunity was considered because it requires the lowest characteristic velocity ($V_{c_{min}} = 14.1$ km/sec compared to $V_{c_{min}} = 14.25$ km/sec for the 1975 opportunity). The 1980 opportunity was selected because it requires the longest Earth-Jupiter flight time for a minimum energy transfer (2.75 years compared with 2.19 years for the 1975 opportunity).

For the 1970 mission, both the minimum energy trajectory and the trajectory for which $V_\infty = V$ were selected for study. The corresponding V_c is 15.2 km/sec (1975 value is $V_c = 15.5$ km/sec). The results are as follows:

- The maximum heliocentric inclination attainable with the minimum energy mission is only 0.5° less than that possible for the 1975 minimum energy mission.

- For all passage inclinations at V_c = 15.2 km/sec, the basic contour (for which $Y_2 = 0$) occurs at slightly higher values of pericenter distance than in 1975. The intercepts of this contour at passage inclinations of 0° and 180° are about 2.2 and 8 Jupiter radii, respectively. Thus, the contour is about 1/8 inch from that shown in figure 6(a).

- Jupiter's radial distance from the Sun at encounter is somewhat greater than during the 1975 opportunity. The orbital velocity is, therefore, somewhat less; hence, V_∞ is also less because of the condition that $V_\infty = V$. This lower value of hyperbolic excess speed is reflected in increased flight times to greater distances. Compared with the 1975 opportunity, the time required to travel to 10 AU is increased by about 6 months. The time to travel to 50 AU is increased by almost 3 years.

For the 1980 opportunity, a characteristic velocity of 17 km/sec was chosen for comparison. Negligible changes were found in the post-encounter trajectories investigated. The location of the basic contour differs at most by 0.2 Jupiter radius, and the flight times to greater distances are essentially unchanged.

CONCLUSIONS

The parametric analysis of these Jupiter swingby trajectories leads to certain basic conclusions. Perhaps the most important of these is the flexibility that becomes available in choosing post-encounter missions if Earth-Jupiter trajectories with characteristic velocities greater than about 15.5 km/sec are used. Missions can be readily performed with solar approach distances that are arbitrarily small and/or with high (greater than 90°) heliocentric inclinations. This is not to say, however, that missions of lower energy are necessarily unattractive. For instance, a minimum energy mission can be used to yield a subsequent heliocentric inclination of almost 30°.

The swingby missions also afford the possibility of solar system exploration far beyond Juipter's orbit. Passage conditions at Jupiter always exist that will permit solar system escape. At the higher energy levels, sizable inclinations can be obtained simultaneously.

For these missions to be practical at all, of course, adequate spacecraft lifetime must be made available. Close solar approaches can be accomplished about 2.5 years after Earth departure, but greater mission flexibility will exist if a lifetime of about 4 years can be realized. Similar mission durations are required for exploration at 10 AU. A lifetime of at least 10 years will be needed to provide a capability for observations at great distances from the Sun. (The example used in this report is 50 AU.)

It would thus appear that a program of extensive solar system exploration using the Jupiter swingbys will require two types of spacecraft. For out-of-ecliptic/solar probe missions, the spacecraft should possess a design lifetime of 2.5-4 years and must have a thermal control system compatible with the

environmental extremes that exist between 5 AU and the selected perihelion distance. For distant exploration, greater lifetime will be needed. The limits on maximum useful distance will be set by the lifetime capability and the power available for communication - the trajectory mechanics themselves pose no constraint.

Finally, the results of the sensitivity analysis indicate that these general conclusions are valid regardless of the particular Earth-Jupiter launch opportunity employed. However, other launch opportunities can affect the post-encounter trajectories enough to warrant detailed study as they become of interest.

National Aeronautics and Space Administration
Moffett Field, Calif., 94035, Dec. 9, 1968
130-06-01-13-15

APPENDIX A

PASSAGE CHARACTERISTICS

Given the initial heliocentric conditions V_1, γ_1 (and $i_1 \equiv 0$), it is necessary to compute corresponding conditions after Jupiter passage, V_2, γ_2, i. Recall the model described earlier for which actual trajectory computations are employed to obtain the Earth-Jupiter heliocentric conic but for which a coplanar model is used to analyze the passage geometry. Since the approach excess speed, V_{∞_1}, shown earlier is not based on this coplanar model, its use would violate the dynamics of the motion within the sphere of influence. Thus, the excess speed must be recomputed within this framework.[1]

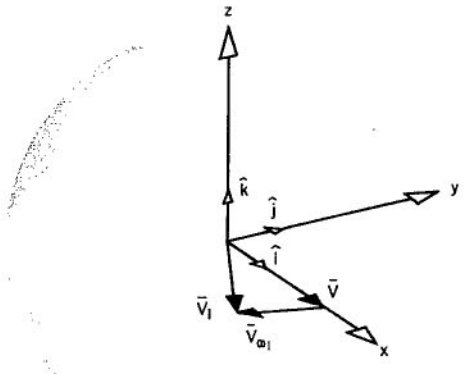

Figure 10.- Derivation of approach excess velocity.

Define a coordinate system (x, y, z) with unit vectors ($\hat{i}$, $\hat{j}$, $\hat{k}$) centered at Jupiter (fig. 10). The x axis is in the direction of Jupiter's orbital speed, V; the y axis is directed toward the Sun; and the z axis is directed toward the north ecliptic pole. Recall that the x-y plane is also defined as Jupiter's equatorial plane. By the definition of hyperbolic excess speed $\bar{V}_{\infty_1} = \bar{V}_1 - \bar{V}$ so that $\bar{V}_{\infty_1} = (\bar{V}_1 \cos \gamma_1 - \bar{V})\hat{i} - \bar{V}_1 \sin \gamma_1 \hat{j}$. The components of a unit vector in the direction of $\bar{V}_{\infty_1}$ are thus;

$$V_{x_1} = \frac{V_1 \cos \gamma_1 - V}{V_{\infty_1}}, \qquad V_{y_1} = -\frac{V_1 \sin \gamma_1}{V_{\infty_1}}, \qquad V_{z_1} = 0$$

Now consider the hyperbolic motion itself. Given $\bar{V}_{\infty_1}$ and inclination, Γ, of the plane of motion with respect to Jupiter's equatorial plane (Γ can take on any value by making the proper midcourse guidance corrections enroute to Jupiter), it is necessary to determine the excess velocity vector at emergence from the sphere of influence, $\bar{V}_{\infty_2}$. This vector is a function of the hyperbolic deflection angle, k, which in turn, is a function of $V_\infty (V_{\infty_1} = V_{\infty_2})$ the pericenter distance, R_p, as follows:

$$\csc \frac{k}{2} = 1 + \frac{RV_\infty{}^2 R_p}{m}$$

where for Jupiter $R/m = 0.5$. Numerical values for k are shown as a function of the relevant parameters in figure 11.

[1] As one would expect, the numerical differences are small. Depending on the characteristic velocity, these computed values are 2-5 percent higher than shown earlier.

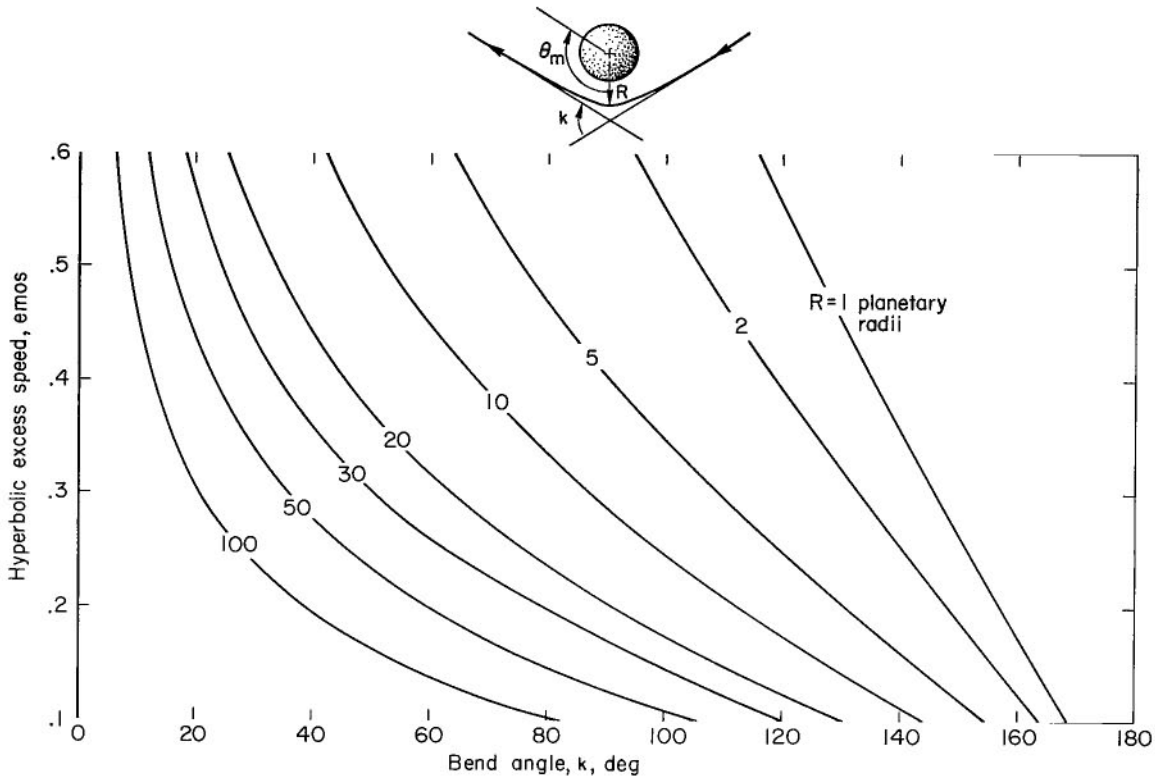

Figure 11.- Hyperbolic asympotote deflection angle at Jupiter.

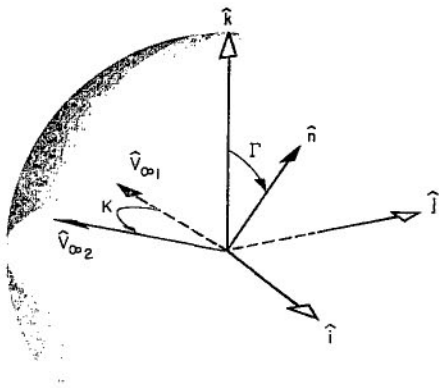

Figure 12.- Derivation of departure excess velocity.

The departure excess velocity vector is found with the aid of figure 12. Here, $\hat{n}$ is a unit vector normal to the plane of the passage hyperbola (i.e., the plane containing V_{∞_1} and V_{∞_2}). The components of $\hat{n}$ are found from the relationships:

$$\hat{n} \cdot \hat{k} = \cos \Gamma$$

$$\hat{n} \times \hat{k} = \sin \Gamma \hat{V}_{\infty_1}$$

which result in the following:

$$n_x = -\sin \Gamma V_{y_1}, \quad n_y = \sin \Gamma V_{x_1}, \quad n_z = \cos \Gamma$$

Consider now the rotation in the plane of motion:

$$\hat{V}_{\infty_1} \cdot \hat{V}_{\infty_2} = \cos k$$

$$\hat{V}_{\infty_1} \times \hat{V}_{\infty_2} = \sin k \hat{n}$$

After a small amount of algebra, the components of the unit vector in the direction of $\overline{V}_{\infty_2}$ are:

$$V_{x_2} = V_{x_1} \cos k - V_{y_1} \sin k \cos \Gamma$$

$$V_{y_1} = \frac{\cos k - V_{x_1} V_{x_2}}{V_{y_1}}$$

$$V_{z_2} = -\sin k \sin \Gamma$$

Since the initial heliocentric velocity after emergence from the sphere of influence is

$$\overline{V}_2 = \overline{V} + \overline{V}_{\infty_2}$$

it follows immediately that,

$$\overline{V}_2 = (V + V_\infty V_{x_2})\hat{i} + V_\infty V_{y_2} \hat{j} + V_\infty V_{z_2} \hat{k}$$

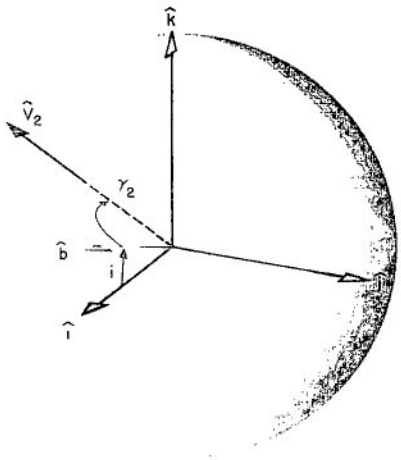

Figure 13.- Derivation of i, γ_2.

The associated path angle, γ_2, and inclination, i, are found with the aid of figure 13. Let $\hat{b}$ represent the $\hat{i}$, $\hat{k}$ components of $\hat{V}_2$. Then

$$\hat{b} \cdot \hat{i} = \cos i$$

so that

$$\cos i = \frac{V + V_\infty V_{x_2}}{\sqrt{(V + V_\infty V_{x_2})^2 + V_\infty{}^2 V_{z_2}{}^2}}$$

By inspection of the figure, we have lastly;

$$\sin \gamma_2 = - \frac{V_\infty V_{y_2}}{V_2}$$

APPENDIX B

POST-ENCOUNTER TRAJECTORIES

At emergence from the sphere of influence, the post-encounter trajectory is described by the initial conditions r_2, V_2, γ_2, i. The remaining elements can be determined readily from the general conic section relationships as follows.

Elliptical Trajectories ($V_2^2 < 2V^2$)

$$a = \frac{r_2}{2 - r_2 V_2^2}$$

$$e^2 = 1 - \frac{r_2}{a}\left(2 - \frac{r_2}{a}\right)\cos^2 \gamma_2$$

$$\cos \theta_o = \frac{a(1 - e^2) - r_2}{e r_2}$$

$$r = \frac{a(1 - e^2)}{1 + e \cos (\theta + \theta_o)}$$

The time, t, in years, to transfer from true anomaly θ_o to true anomaly $\theta + \theta_o$ is found from the following expression:

$$t + t_o = \frac{a^{3/2}}{2\pi}\left\{2 \tan^{-1}\left[\left(\frac{1-e}{1+e}\right)^{1/2} \tan\left(\frac{\theta + \theta_o}{2}\right)\right] - \frac{e(1 - e^2)^{1/2} \sin (\theta + \theta_o)}{1 + e \cos (\theta + \theta_o)}\right\}$$

where t_o is the time that would have been required to transfer from perihelion to θ_o.

The heliocentric latitude, η, as a function of θ is simply,

$$\sin \eta = \sin i \sin \theta$$

Hyperbolic Trajectories ($V_2^2 > 2V^2$)

$$a = \frac{r_2}{r_2 V_2^2 - 2}$$

$$e^2 = 1 + \frac{r_{2_4}}{a}\left(2 + \frac{r_{2_4}}{a}\right)\cos^2 Y_2$$

$$\cos \theta_o = \frac{a(e^2 - 1) - r_{2_4}}{e r_{2_4}}$$

$$r = \frac{a(e^2 - 1)}{1 + e \cos (\theta + \theta_o)}$$

The limiting true anomaly (true anomaly of a hyperbolic asymptote) is simply:

$$\cos \theta_m = -\left(\frac{1}{e}\right)$$

so that the maximum transfer angle after encounter is:

$$\theta_{max} = \theta_m - \theta_o$$

Finally the transfer time is

$$t + t_o = \frac{a^{3/2}}{2\pi}\left\{\frac{e(e^2-1)^{1/2} \sin (\theta+\theta_o)}{1 + e \cos (\theta+\theta_o)} - \ln\left[\frac{1 + \left(\frac{e-1}{e+1}\right)^{1/2} \tan\left(\frac{\theta+\theta_o}{2}\right)}{1 - \left(\frac{e-1}{e+1}\right)^{1/2} \tan\left(\frac{\theta+\theta_o}{2}\right)}\right]\right\}$$

REFERENCES

1. Mascy, Alfred C.: 1.0 AU Extra-Ecliptic Constant Low-Thrust Missions. AIAA paper 68-546, June 1968.

2. Meissinger, H. F.; Park, R. A.; and Hunter, H. M.: A 3-kw Solar-Electric Spacecraft for Multiple Interplanetary Missions. J. Spacecraft and Rockets, vol. 5, no. 6, June 1968, pp. 678-85.

3. Mascy, Alfred C.; Dugan, Duane W.; and Pitts, Samuel W.: Applications of Combined Electric, High-Thrust Propulsion Systems. J. Spacecraft and Rockets, vol. 5, no. 7, July 1968, pp. 785-91.

4. Hunter, Maxwell W., II: Future Unmanned Exploration of the Solar System. Astronautics and Aeronautics, vol. 2, no. 5, May 1964, pp. 16-26.

5. Deerwester, Jerry M.: Jupiter Swingby Missions to the Outer Planets. J. Spacecraft and Rockets, vol. 3, no. 10, Oct. 1966, pp. 1564-7.

6. Niehoff, John C.: A Survey of Multiple Missions Using Gravity Assisted Trajectories. IIT-M-12, IIT Research Institute, NASA CR-76767, 1966.

7. Klopp, David A.; and Niehoff, John C.: The Accessible Regions Presentation of Gravity - Assisted Trajectories Using Jupiter. IIT-T-18, IIT Research Institute, NASA CR-87495, 1967.

8. Anon.: Trajectories to Jupiter, Ceres, and Vesta. Planetary Flight Handbook, vol. III, pt. 5, NASA SP-35, 1966.

NASA-Langley, 1969 —— 30 A-3224

"The aeronautical and space activities of the United States shall be conducted so as to contribute . . . to the expansion of human knowledge of phenomena in the atmosphere and space. The Administration shall provide for the widest practicable and appropriate dissemination of information concerning its activities and the results thereof."

— NATIONAL AERONAUTICS AND SPACE ACT OF 1958

NASA SCIENTIFIC AND TECHNICAL PUBLICATIONS

TECHNICAL REPORTS: Scientific and technical information considered important, complete, and a lasting contribution to existing knowledge.

TECHNICAL NOTES: Information less broad in scope but nevertheless of importance as a contribution to existing knowledge.

TECHNICAL MEMORANDUMS: Information receiving limited distribution because of preliminary data, security classification, or other reasons.

CONTRACTOR REPORTS: Scientific and technical information generated under a NASA contract or grant and considered an important contribution to existing knowledge.

TECHNICAL TRANSLATIONS: Information published in a foreign language considered to merit NASA distribution in English.

SPECIAL PUBLICATIONS: Information derived from or of value to NASA activities. Publications include conference proceedings, monographs, data compilations, handbooks, sourcebooks, and special bibliographies.

TECHNOLOGY UTILIZATION PUBLICATIONS: Information on technology used by NASA that may be of particular interest in commercial and other non-aerospace applications. Publications include Tech Briefs, Technology Utilization Reports and Notes, and Technology Surveys.

Details on the availability of these publications may be obtained from:

SCIENTIFIC AND TECHNICAL INFORMATION DIVISION

NATIONAL AERONAUTICS AND SPACE ADMINISTRATION

Washington, D.C. 20546